Key Engineering Materials *Online: 2012-12-27*
ISSN: 1662-9795, Vol. 533, pp 53-90
doi:10.4028/www.scientific.net/KEM.533.53

Cold Spraying of Titanium: A Review of Bonding Mechanisms, Microstructure and Properties

T. Hussain[1]

[1] Centre for Energy and Resource Technology (CERT), School of Applied Sciences,

Cranfield University, Bedford, MK43 0AL, UK

[1]t.hussain@cranfield.ac.uk

Keywords: cold spray, deposits, bonding mechanisms, titanium

Abstract. Cold gas dynamic spraying (CGDS) is a relatively new branch of surface engineering that involves modification of the surface of substrates to provide specific engineering advantages, which the substrate alone cannot provide. Cold spraying, as a metal deposition technique, involves spraying of typically 10-40 μm particles which are accelerated by a propellant gas to 300- 1200 m/s at a temperature well below the melting point of material, and upon impact deform and adhere to the substrate. The deposition process in cold spraying occurs in a solid state which results in reduced oxidation and absence of phase changes; whereas, in thermal spraying deposition occurs of molten or semi molten particles. Over the last decade the interest in cold spraying has increased substantially. Considerable effort has been invested in process developments and optimization of coatings like copper. However, bonding in cold spraying is still a matter of some debate. The most prevalent theory is that when a particle travels at a minimum required velocity the particle deforms at a very high strain rate upon impact and during this deformation thermal softening dominates over work hardening in impact zone and a material jet is produced. This material jet removes oxides from the surface of the materials and the metal-to-metal contact is established between the freshly exposed surfaces. However, precisely how this high strain rate deformation behaviour of material promotes bonding is still unclear and requires further investigations. This article provides a comprehensive review of the current theories of bonding in cold spraying based on numerical modelling of impact and experimental work. The numerical modelling of the impact section reviews adiabatic shear instability phenomena, critical velocity, critical particle diameter, window of deposition of particles, particle impact on various substrates and the role of adhesion and rebound energy. The review of the experimental section describes the shear lip formation, crater formation on the substrates, role of surface oxides, characterization of bond formation, role of substrate preparations, coating build up mechanisms and contributions of mechanical and metallurgical components in bonding.

Cold spraying of copper and aluminium has been widely explored in the last decade, now it is of growing interest to the scientific and engineering communities to explore the potential of titanium and its alloys. Titanium and its alloys are widely utilized in many demanding environments such as aerospace, petrochemical, biomedical etc. Titanium components are very expensive to manufacture because of the costly extraction process of titanium and their difficult to machine properties. Therefore, additive manufacturing from powder and repair of titanium components are of great interest to the aerospace industry using technologies such as cold gas spraying. Titanium coating as a barrier layer has a great potential for corrosion resistant applications. Cold spraying has a great potential to produce oxygen-sensitive materials, such as titanium, without significant chemical degradation of the powder. In-flight oxidation of materials can be avoided to a great extent in cold spraying unlike thermal spraying. This review article provides a critical overview of deposition efficiency of titanium powder particles, critical velocity, bond strength, porosity, microhardness, microstructural features including microstrain and residual stress, mechanical properties reported by various research groups. A summary of the competitor warm sprayed titanium coating is also presented in this article.

Contents

1 Introduction

Cold Gas Dynamic Spray (CGDS) was first developed by Papyrin et al. [1] in the mid- 1980s at the Institute of Theoretical and Applied Mechanics of the Russian Academy of Science in Novosibirsk while working with tracer particles in supersonic wind tunnels. Since then several research groups across the world have been developing the process as a surfacing/ near-net shape metal deposition technique. Cold spray is a high rate material deposition process in which powder particles are accelerated in a supersonic jet of compressed gas to high velocities, whereupon impact with a substrate/previously deposited layer, deform plastically, and bond to the surface. The high velocity supersonic gas jet is produced by use of a converging-diverging de Laval nozzle. In the last decade, a number of cold spray research groups from all over the world: Japan, South Korea, Canada, USA, Russia, Germany, Finland, UK, Australia, India, and China have been active in developing new cold spraying systems to spray challenging powder feedstock, optimizing process parameters and investigating the bonding mechanisms in cold spraying.

This review article provides a comprehensive overview on working principles of cold spraying and the current theories of bonding mechanisms based on experimental work and numerical modelling of impact. An overview of the properties of cold-sprayed titanium coatings/deposits and the role of different process parameters on coating performance is a specific focus. The terms cold sprayed titanium “coatings” and “deposits” have been used interchangeably throughout this article.

1.1 Thermal spraying

Thermal spraying is a generic term for applying metallic and non-metallic coatings in which the molten or semi- molten particles are deposited onto a substrate [2]. In thermal spraying, the particles are heated and accelerated towards a substrate onto which a coating is formed. The combination of high particle temperature and/or high particle velocity results in forming a deformed splat on the substrate. Deposition of successive splats causes a coating thickness from a few microns to few millimetres to be builtup on the substrate. Thermal spray processes can be grouped into three broad categories: flame spray, electric arc spray and plasma arc spray [2]. Different energy sources (i.e., flame, electric arc and plasma) are used to melt the coating materials (in powder, wire or rod form) and propel them towards the substrate. The key advantage of thermal spraying is that material or composites which partially melt without decomposing can be sprayed. Fig. 1 compares the particle velocity and gas temperature of different thermal spray processes. Flame spray includes low velocity powder flame, wire flame and high velocity oxy-fuel (HVOF) methods where the gas temperature is relatively low. In flame spray, the coating material is aspirated into the oxy-fuel stream, heated and carried by the flame towards the substrate [2]. In arc (wire) spray process, two consumable wire electrodes are fed into the gun. This creates an arc between them which melts the tip of the wire. The molten metal is then atomized by a gas stream and propelled towards the substrate. The velocity of the particles is low and the temperature is higher than flame spray processes [2]. However, in plasma spray process, the powder heating region

is from 2500 °C to 14000 °C, significantly above the melting point of any known material. Typically argon or argon-hydrogen mixture is heated by a dc arc to produce the plasma [2]. A range of materials including ceramics can be sprayed using plasma spray.

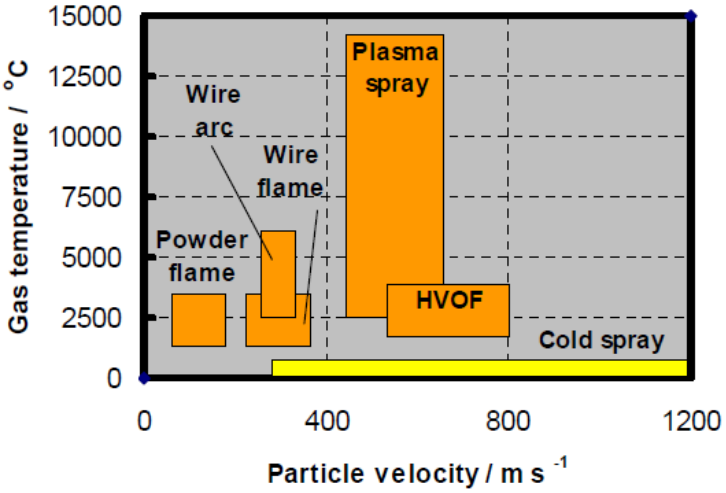

Fig. 1 Temperature/ velocity regimes for thermal spray and cold spray processes [3]

Commercially pure grade of titanium can be applied using various thermal spraying techniques (e.g., HVOF, plasma, shrouded arc spraying etc). In all thermal spraying techniques, titanium feedstock is heated to molten/ semi-molten state and propelled towards the substrate to be coated. Oxidation of titanium particles can readily occur during heating due to the high affinity of titanium for oxygen, which can also affect its final properties. To eliminate this problem, inert atmospheres or vacuum need to be employed which increases cost of the process and reduces flexibility. In addition, thermal spraying of titanium result in tensile residual stresses on the top of the coating due to coating- substrate mismatch of cooling rates. Tensile residual stresses can result in crack growth and de-lamination of the coatings.

1.2 Cold spraying

Cold spraying is a high strain-rate material deposition technique, in which powder particles (typically 10 - 40 μm in size) are accelerated to speeds of between 300-1200 m/s, and upon impact with a substrate (or previously deposited particles), deform plastically and adhere [4-7]. The process is also referred to as cold gas dynamic spray because the process utilizes gas dynamic principle of helium or nitrogen as an accelerating gas. Deposition rates up to 14 kg/ h have also been reported in the literature [2]. Fig. 2 shows, schematically the cold gas dynamic spraying process. In this process, a high pressure gas (helium or nitrogen) supply is used to accelerate the powder particles. A high pressure powder feeder is used to introduce the powder in the high pressure gas stream. In some systems, a gas heater is used to increase the temperature of the gas to further accelerate the particles. The key component of a typical cold spray process is a convergent-divergent nozzle termed a de Laval nozzle, which accelerates the gas supersonically and gives the particles their required velocity to deposit onto a substrate. In a de laval nozzle, there are two sections: a convergent section and a divergent section. In some cold spray system (Kinetic Metallization, Inovati Ltd) a convergent barrel nozzle is used where the flow is restricted to Mach 1.

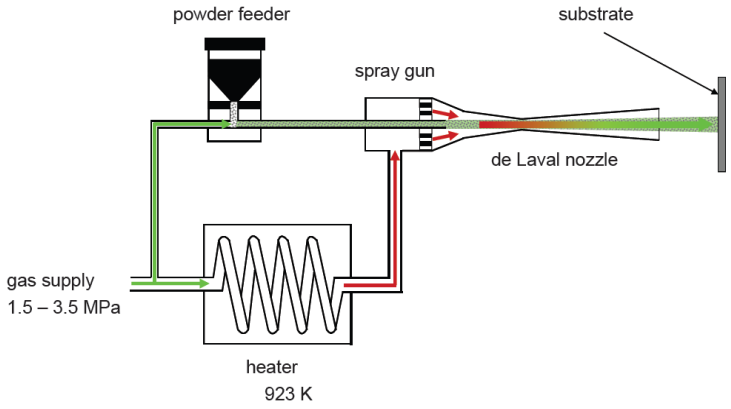

Fig. 2 Schematic of a cold gas dynamic spray system [7]

There are two different types of commercially available cold spraying equipments: high pressure cold spraying system and low pressure cold spraying system (LPPS). Commercial high pressure cold spraying systems are manufactured by Cold Gas Technology (CGT) GmbH (Ampfig, Germany). The latest model of Kinetiks 4000/47 from CGT can achieve a pressure of 4.0 MPa with a process gas temperature of 800˚C. A 47 kW heater is used as a primary gas heater and a 17 kW gun heater is used in combination with the primary gas heater. Kinetiks 4000 utilizes a WC nozzle with an elongated pre-chamber for powder mixing with the gas and can deposit high end materials like titanium, tantalum etc. There is also a portable version of the high pressure cold spray system called Kinetiks 2000 which operates below 2.0 MPa and up to 400˚C. This portable cold spray system is mainly used for on-site repair purposes using light materials like aluminium, copper, zinc, tin, magnesium etc [8].

Inovati Ltd (Santa Barbara, CA, USA) manufactures commercially available cold spraying model called Kinetic Metallization (KM). The Kinetic Metallization Coating Development System (KM-CDS) 3 is a fully integrated system with a 6+1 axis robot for coating development. KM-CDS model can achieve a gas temperature of 370˚C while working at 1.0 MPa inlet pressure. The system utilizes friction compensated sonic nozzle made from cemented carbide for the deposition. A 2.5 kW thermal conditioning unit is integrated with the nozzle. There is also a portable version called Mobile Coating Systems (MCS) which is used for onsite repair work [9].

Supersonic Spray Technology (SST), which is a division of Centerline Ltd, manufactures commercially available low pressure cold spray systems. The low pressure Dymet model utilizes pressures below 1.0 MPa and a gas temperature below 600˚C for coating deposition. The powders used in this low pressure cold spraying system typically include ceramics which helps in hammering the particles and thus facilitating particle deposition. In contrast to high pressure system where powder is introduced at the converging section of the nozzle, in this low pressure cold spray system the powder is introduced at the diverging section of the nozzle [10].

In the cold spraying process, the gas and particle temperatures remain well below the melting temperature of the spray materials and therefore the particles are in solid state, and formation of coatings occurs due to the kinetic energy of the particles on impact [7]. Unlike thermal spraying, where the particles are molten or semi molten, the deposition of particles in the solid state by cold spraying has various advantages. Some of the key advantages of cold spray are mentioned as follows [11].

- High deposition efficiency, values as high as 100% for titanium [12] and copper have been reported.
- High deposition rate, up to 14 kg/ h for various materials [2].

- Substrate preparation by grit-blasting is not required for ductile materials as the process can be viewed as a combination of grit-blasting, spray coating and shot peening [11].
- Low porosity coating because of visco-plastic deformation of the particles during deposition [7]. Also the particles from the trailing edge of the moving plume sputter away any loosely bonded particles and shot-peen the underlying layer to reduce porosity.
- Minimal thermal input to the substrate because of the absence of any high temperature jet to heat the substrate.
- Compressive residual stress in the coating because of plastic deformation in the solid state, which enhances fatigue properties of the coating.
- No phase change, no oxidation and no grain growth due to a lack of heating of the powders.
- High thermal and electrical conductivity of coatings can be produced from metals ,like copper, due to a low porosity and negligible oxide [13].
- High strength and hardness of the cold sprayed coatings compared to the bulk material because of the high degree of plastic deformation of the particles [14].
- In addition, corrosion resistant coating like tantalum [15] and aluminium [16] produced from cold spraying showed bulk like properties in corrosion tests.

2 Gas dynamic principles in cold spraying

The convergent- divergent nozzle or de Laval nozzle is a key component in the cold spraying system. High pressure gas is fed into the back of the convergent section of a de Laval nozzle. Fig. 3 shows the schematics of a de Laval nozzle used in cold spraying. In a de Laval nozzle the flow can be accelerated or decelerated by changing the flow areas [17, 18]. The compressible nature of a gas allows the de Laval nozzle to operate. At the throat of the nozzle, the gas reaches sonic condition (Mach no. =1) when the flow is chocked (i.e., it has reached the maximum possible mass flow rate). At the divergent section of the nozzle, the gas continues to accelerate to supersonic velocities. As the gas accelerates in the divergent section of the nozzle, the temperature and pressure decrease from their original stagnation values [17]. The particles accelerate as they pass along the nozzle gaining kinetic energy from the supersonic gas [19].

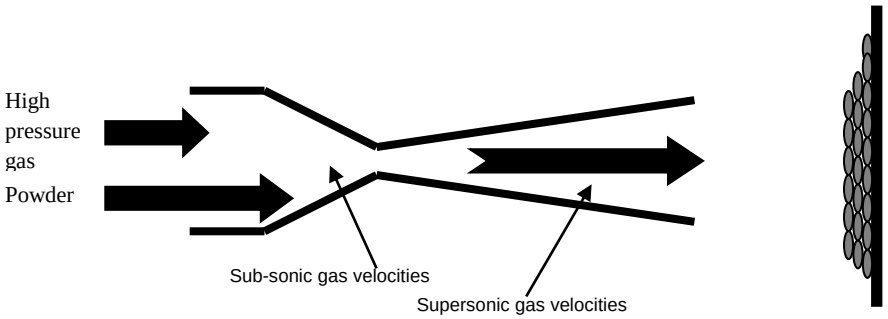

Fig. 3 Schematics of a cold gas dynamic spray de Laval nozzle [19]

The readers are referred to the following references [17, 20-22] for a comprehensive analysis of gas dynamic equations related to cold spraying. The velocity of the particles in cold spraying is affected by the type of gas used, gas pressure and gas temperature. A convenient way of increasing the gas velocity is to use a gas with lower molecular weight (such as helium) or to increase the gas temperature [23]. In general, particle velocity increases with the decrease of particle size and a particle of lower density under the same conditions will reach a higher velocity [24-26]. However, this high velocity of smaller particles does not necessary contribute to deposition in cold spray due to bow shocks, external to the nozzle.

Interaction of particles with the substrates from a fluid mechanics point of view in the cold spraying has been subjected to much research [21, 25, 27-31]. Shockwaves occur as a result of the adjustment of a supersonic flow to downstream conditions [28].When the gas molecules impact the substrate, there is a change in energy and momentum, and the pressure waves form a normal shock wave. Since the substrate is perpendicular to the gas flow, the deflection angle is greater than maximum deflection angle for an oblique shockwave and as a result the shockwave is curved and detached- which is called a bow shock [28]. The bow shock reduces the velocity of the gas and that of the entrained particles. If the particles are too large and heavy, they will not be accelerated enough within the nozzle, but the deceleration will be modest in the bow shock zone. However, if the particles are too small and light, they might acquire a high velocity but may be decelerated in the bow shock zone [21, 32]. By increasing the standoff distance the effect of bow shock can be decreased and deposition performance can be increased. However, if the standoff is increased beyond an optimum distance the deposition efficiency is decreased due to a decrease of particle velocity [25].

3 Bonding mechanisms in cold spraying

The mechanism of bonding in cold spraying is a matter of some debate. A number of hypotheses have been proposed concerning the mechanism by which bonding takes place in cold spraying. The bonding studies undertaken by various researchers in the field can be divided into two categories: mathematical modelling of impact using numerical methods of investigations and experimental investigations using microstructural characterization techniques.

3.1 Mathematical modelling using numerical methods

A number of studies on numerical simulation of particle deformation during the cold spraying process have been reported in literature [4, 6, 7, 33-46]. The key findings of their studies will be outlined and the proposed bonding theories will be discussed here. The high strain rate material behaviour in the numerical simulations are described by the well known Johnson-Cook plasticity model which accounts for strain hardening, strain rate hardening and thermal softening of materials [47]. Finite element simulation software ABAQUS Explicit has been widely used in simulating the particle deformation in cold spraying. In addition, the CTH code developed at Sandia National Laboratories for multi-material, large deformation, strong shockwave, solid mechanics cases was also used to simulate the cold spraying process [35].

3.1.1 Finite element modelling of single particle impact of copper

In cold spraying when a spherical particle, travelling at or above the critical velocity, impacts a substrate, a strong pressure field propagates spherically into the particle and substrate from the point of contact. As a result of this pressure field, a shear load is generated which accelerates the material laterally and causes localized shear straining. The shear loading under critical conditions leads to what is termed as adiabatic shear instability where thermal softening is locally dominant over strain and strain rate hardening, which leads to a discontinuous jump in strain and temperature and breakdown of flow stresses [6]. This adiabatic shear instability phenomenon results in viscous flow of material in an outward flowing direction at temperatures close to the melting temperature of the material. This material jetting is also a known phenomenon in explosive welding of materials. The evidence for this material jetting phenomenon is shown in Fig. 4 which shows SEM images of a bonded particle with a ring of jet type morphology around the impact zone.

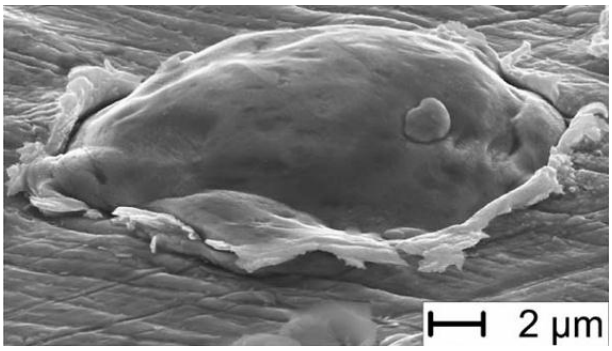

Fig. 4 SEM of a copper particle on a copper substrate [7]

Fig. 5, from the work of Assadi et al.[7], shows the temporal development of plastic strain, temperature and flow stress at a point on copper particle which went through the highest amount of deformation (jetting) upon impacting a copper substrate for four different impact velocities. When the impacting velocity of the copper particle was 580 m/s there was a significant jump in strain up to a value of 10, which is different from the strain curves for other velocities. A material suitable for cold spray should withstand such severe conditions of plastic flow without fracturing[6]. The increase in velocity possibly changed the material deformation mechanism from plastic to viscous (Fig. 5a). Similarly, for velocity of 580 m/s the temperature was significantly higher and approached the melting temperature of copper (Fig. 5b). Fig. 5c shows the temporal evolution of stress during the deformation of the particle. For the velocity of 580 m/s, after 0.03 µs there is a breakdown of stress which coincides with the increase of strain and temperature. This breakdown of stress could be due to thermal softening of the material. When the material approaches the melting temperature, the shear strength is lost which results in excessive deformation (i.e. jetting) of the material. This jump in strain and temperature and breakdown of stress is defined as adiabatic shear instability phenomena [7]. Moreover, experimentally determined critical velocity of an inert gas atomized copper powder (-5 +22 µm) was 570 m/s [7].

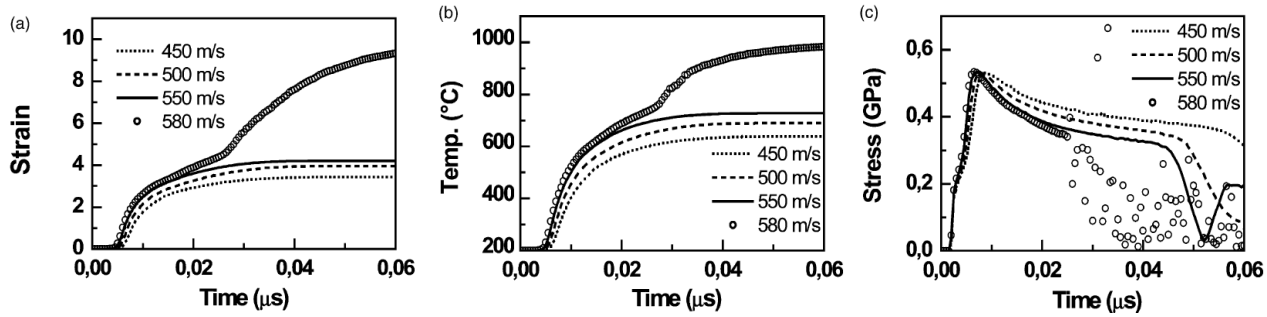

Fig. 5 Calculated temporal development of (a) plastic strain (b) temperature and (c) flow stress at a critical node of sprayed Cu particle from FE on Cu substrate modelling [7]

Although a number of publications infer that adiabatic shear instability phenomena leads to bonding in cold spraying, but the physical mechanism by which adiabatic shear instability promotes bonding is not clear. It is argued that the adiabatic shear instability leads to more oxide removal on the contact surfaces and when the two oxide free surfaces come in contact a metal-to-metal bonding can form. Metal-to-metal bonding is also found in other solid state processes such as cold welding or roll bonding [48]. The key criteria separating cold spray bonding from other solid state processes is the strain rate; stain rate in cold spraying is the range of 10^{6-9} /s. It is unlikely for adiabatic shear instability to take place in cold welding or roll bonding; however, there is large plastic strain at the

interface. Bonding theories on cold welding suggest that if sufficient pressure for plastic deformation is present at the interface it will lead to conformal contact (e.g., atoms are separated by roughly one atomic spacing) along a substantial portion of the interface. Adhesion on the nano scale involves atomic interactions between the contacting clean interface and high contact pressures to make the surfaces mutually conforming. The removal of surface oxides by a material jet produced by adiabatic shear instability can in principle, provide clean surface for adhesion between two mutually conforming regions [4]. It is critical to have a sufficient number of available slip systems in the material to create conformal contact [49]. In friction studies of materials it was reported that interfacial bonding is enhanced when the crystal structure of the metal is FCC instead of HCP or BCC, due to the large number of active slip systems in FCC. Numerical models in cold spraying are helpful at predicting the material deformation behavior but the current models do not take into account of any oxide removal or conformal contact between two surfaces.

3.1.2 Critical impact velocity and critical particle diameter

An adiabatic shear instability occurs when particles travel at a sufficiently high velocity called the critical velocity [6, 7, 21, 44]. Fig. 6 shows the proposed schematic relationship between deposition efficiency and particle velocity. Deposition efficiency is the mass ratio of deposited to impacting particles. Particles travelling below a certain velocity will result in abrasion of the substrate upon impact. However, particles travelling at or above that certain velocity will result in deposition and coating formation. These relationships lead to the proposal of a cut-off velocity called critical velocity, below which abrasion occurs and above which deposition occurs [26].

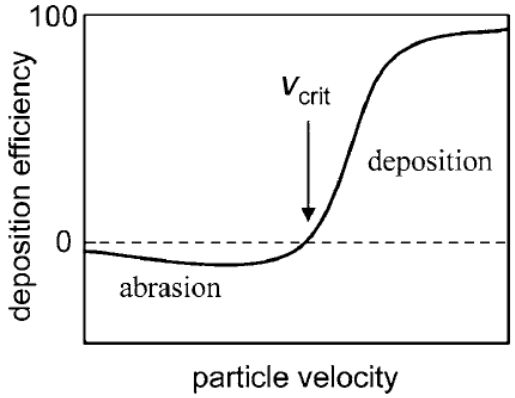

Fig. 6 Schematic of relationship between particle velocity and deposition efficiency proposed by Gartner et al. [26]

An equation of the critical velocity taking into account of the material properties was proposed by Assadi et al. [7].

$$V_{cr} = 667 - 14\rho_p + 0.08T_m + 0.1\sigma_u - 0.4T_i \quad (1)$$

Where, ρ_p is the density in g/cm^3, T_m is the melting temperature in °C, σ_u is the ultimate tensile strength in MPa and T_i is the initial particle temperature in °C. It can be seen from that equation that critical velocity increases with increasing yield strength and melting temperature and decreases with increasing density and particle temperature. [7].Later, Schmidt et al. [6] provided another equation to calculate the critical velocity of particles using energy balance theories.

$$V_{cr} = \sqrt{\frac{F_1 4\sigma_u \left(1 - \frac{T_i - T_R}{T_m - T_R}\right)}{\rho_p} + F_2 c_p (T_m - T_i)} \quad (2)$$

Where F_1=1.2 and F_2=0.3 are calibration factors, T_R is reference temperature (293 K) and σ_u is the tensile strength of the material. Fig. 7 shows the results for calculation of critical velocities for 25 μm particles for different materials. Schmidt's equation provides a better agreement with the experimentally determined critical velocities. This equation provides more accurate prediction of critical velocity for materials like tin and tantalum over Assadi's equation.

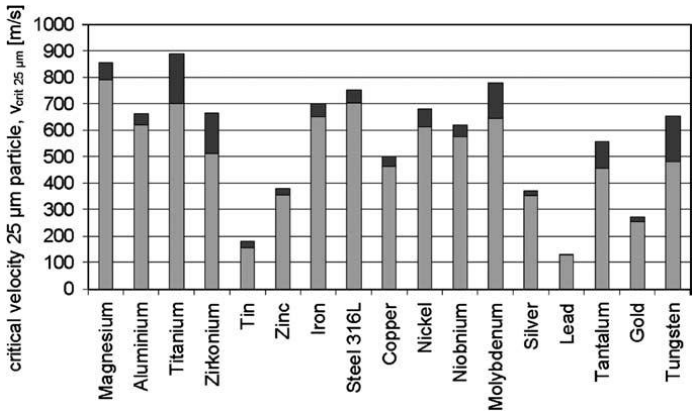

Fig. 7 Critical impact velocity for a 25 μm particle calculated using Schmidt's equation [6]. The dark grey level indicates the range of uncertainity

Semi-empirical determination of critical velocity is performed by measuring the velocity distribution combined with the measured deposition efficiency and the particle size distribution to calculate the size and the velocity of the largest particle which would bond to the substrate. The corresponding velocity of this largest and slowest bonded particle is taken as the experimentally determined critical velocity [6, 7, 30].

The sizes of the particles also influence the critical velocity [6]. Following the adiabatic shear instability phenomenon, i.e., rapid increase in localized temperature at the bond zone, the rate at which the material loses heat plays an important role in bonding. The cooling rate of the material decreases with increasing particle size. The cooling rate has to be "low enough" to promote shear instability and on the other hand, "high enough" to let the interface solidify and finish the bonding process. Shear instability can be hindered in very small particles due to high temperature gradients and higher strain rate hardening due to a higher strain rate in the small particle. Moreover, smaller particles are exposed to higher quench rates during production which might result in a higher strength and due to higher surface to volume ratio smaller particles will have higher impurity. All these will hinder localized deformation at the onset of adiabatic shear instability and thus increase the critical velocity. Schmidt et al. proposed the following equation for critical dimension of particles

$$d_{crit} = 36 \frac{\lambda_p}{c_p \cdot \rho_p \cdot V_p} \quad (3)$$

where λ_p is the thermal conductivity and c_p is the specific heat of the particle. This equation signifies a critical dimension of particle above which thermal diffusion is slow enough for adiabatic shear instability to occur for an impacting particle. Fig. 8 shows the critical diameter of different particles measured using the equation and particle sizes smaller than the critical dimension will not reach adiabatic shear instability criterion.

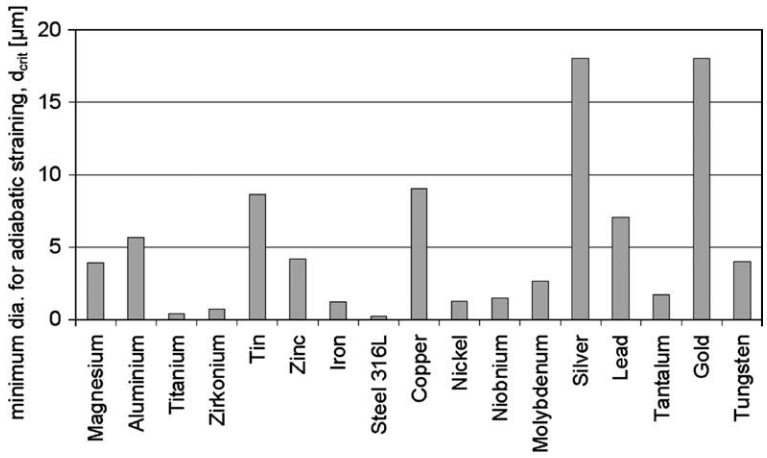

Fig. 8 Minimum particle diameter for localized adiabatic shear instability for different materials [6]

3.1.3 Window of deposition in cold spraying

Fig. 9 shows the proposed variation in deposition efficiency with particle velocity at a certain temperature [43, 44]. It is argued that at 50% deposition efficiency the corresponding velocity should be defined as the critical velocity [43]. For a ductile spraying material, deposition efficiency increases sharply following increase of the velocity beyond critical velocity reaching a saturation 100% deposition efficiency [43]. Optimum coating conditions can be expected at a region where deposition efficiency is nearly 100%. Beyond the saturation point, increase in particle velocity results in a decrease in deposition efficiency due to hydrodynamic erosion of particles [43, 50]. Cross-sectional images of large scale impact of a 20 mm copper ball impacting a low carbon steel are also shown in Fig. 9 to illustrate the effect of this phenomenon. The velocity of the particles beyond which no deposition occurs (0% DE) and only results in erosion is defined as erosion velocity. In addition, erosion velocities of different materials can be calculated using Schmidt's equation with factors, F_1=4.8 and F_2= 1.2. The range of velocities between critical velocity and erosion velocity is a window where material deposition can occur in cold spraying [51]. Brittle materials, like ceramic will result in erosion at any velocity which makes it difficult to deposit using cold spraying.

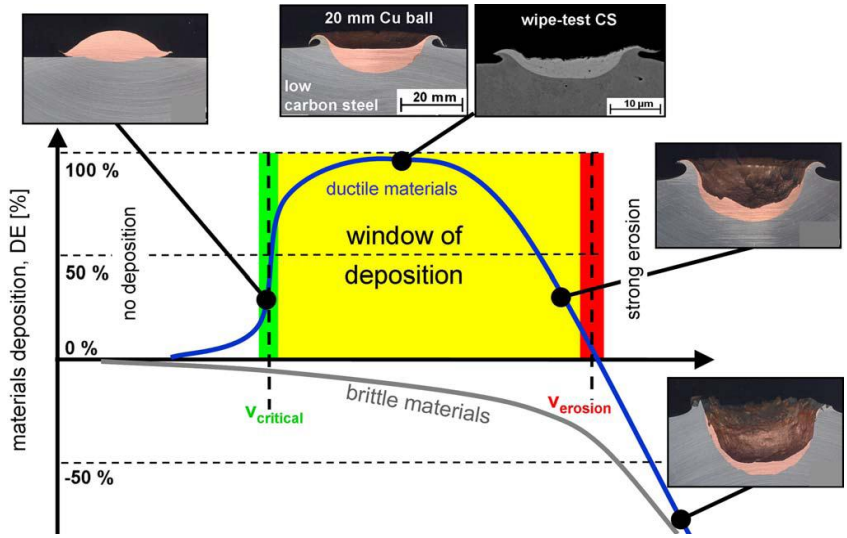

Fig. 9 Schematic correlation between particle velocity, deposition efficiency and impact effects at constant temperature [43, 44]

3.1.4 Particle-substrate impact behaviour

Deformation behaviour of particle-substrate in cold spraying can be divided into four categories : soft particle on soft substrate, soft particle on hard surface, hard particle on soft substrate and hard particle on hard surface [34]. Fig. 10 shows the four cases of such particle impact onto substrates. In the case of soft particle /soft substrate (Al/Al), large deformation is observed as compared to hard particle /hard substrate (Ti/Ti) due to low material strengths in the former case. In both cases, higher temperature was found at the substrate side as compared to the particle side. In the other two cases of soft particle /hard substrate (Al/mild steel) and hard particle /soft substrate (Ti/Al), the deformation occurred in the relative soft counterpart. In addition, a much higher temperature was achieved in the softer side. Bae et al. classified 22 materials combination into the above four different categories and reported a detailed study on critical velocities, critical sizes, contact areas and contact time in reference [34].

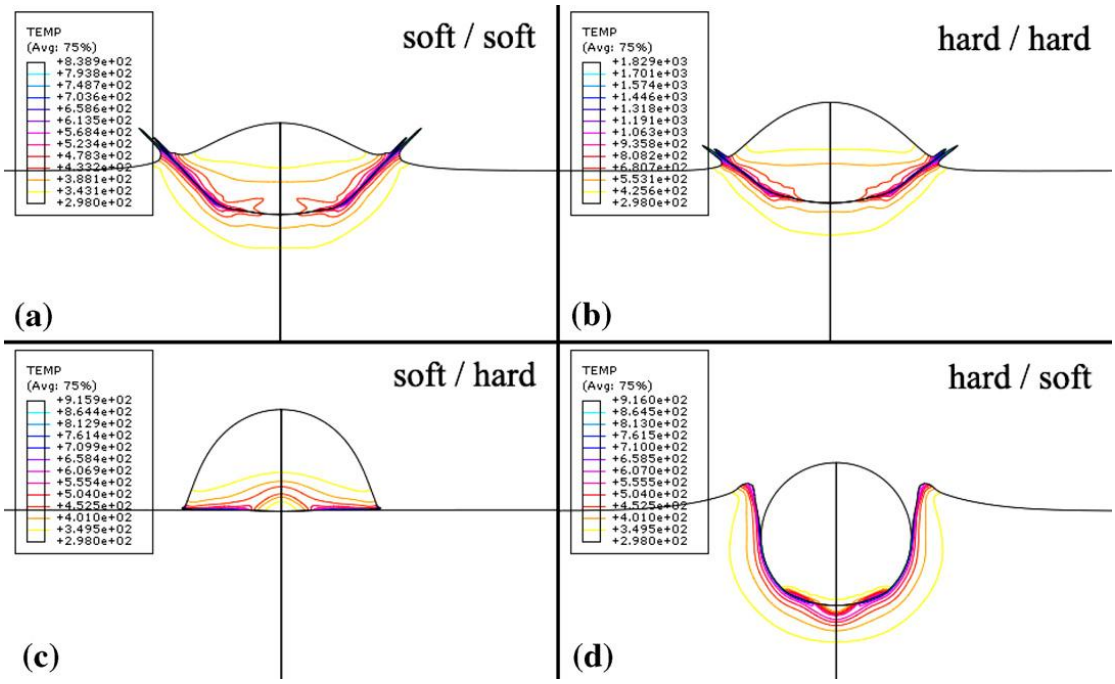

Fig. 10 Four cases of particle impact onto substrate (a) soft/soft (Al onto Al at 775 m/s) (b) hard/hard (Ti onto Ti at 865 m/s) (c) soft/hard (Al onto mild steel at 365 m/s) (d) hard/soft (Ti onto Al at 655 m/s) [34]

A number of numerical simulations on multiple particle impact behaviour in coating formation have been studied and it was found that the interaction between particles during deposition plays an important role in particle deformation and coating formation [31, 33, 52]. Also, the role of different simulation methods in multiple particle impact modelling using Eulerian method, Lagrangian method and smoother particle hydrodynamics methods (SPH) showed that the the Eulerian method provided results comparable to the experimental investigations [52].

A parameter called thermal boost up zone (TBZ) was introduced to quantitatively differentiate between adiabatic shear instability phenomena in dissimilar particle-substrate [33, 34, 53]. Fig. 11 shows that when the particle is undergoing localized deformation after a transition point a rapid increase in temperature takes place, marking the onset of adiabatic shear instability. The TBZ is theoretically defined as follows

$$TBZ\ (Z_{tb}) = H_{tb}.W_{tb} = [(T_{max}-T_r)/T_m][(t_c-t_i)/t_c] \quad (4)$$

Where T_{max} is the maximum temperature, T_r is the temperature of transition point, Tm is the melting temperature, t_i is the incubation time and t_c is the total contact time. In short, H_{tb} is defined as normalize TBZ height and W_{tb} is defined as normalized TBZ width.

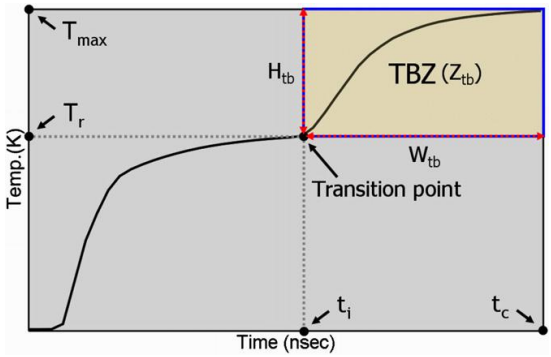

Fig. 11 Schematics of thermal boost up zone (TBZ) [34]

In Cu particle impacting a Cu substrate, there is a large TBZ (i.e., large H_{tb} and W_{tb}). However, in the cases of a soft particle impacting on a soft substrate (Al-Al) and a hard particle impacting on a hard substrate (Ti-Ti) the TBZ width (W_{tb}) and TBZ height (H_{tb}) are much smaller compared to the Cu-Cu system. On the contrary, when a soft particle impacts on a hard substrate (Al- Mild Steel) and a hard particle impacts on a soft substrate (Ti- Al) the heating up rate is so high that no "transition point" is observed and hence no well defined TBZ can be established. As a result, the flow stresses collapse to zero sharply. Rapid and severe deformation of the softer counterpart is considered to be the reason for the rapid changes in temperature and flow stresses. The highly saturated temperature and low flow stresses found in hard/soft or soft/hard cases result in high adhesion and low rebound energy, increasing the chance of successful bonding.

3.1.5 Adhesion and rebound energy

A bonding model consisting of adhesion energy and rebound energy exists in cold spraying literature [54]. In the model bonding is considered to be a result of a competition of adhesion energy and rebound energy. The authors experimentally observed the effect of velocities in deposition over a wide range (i.e., below critical velocity and above erosion velocity). Adhesion energy (Ad) is defined as the energy required to detach a bonded particle from the substrate. Ad=a% Ad_{max}, where Ad_{max} is the maximum adhesion energy and a% is the fraction of bonded atoms per unit of adhesive interface. Kurochkin et al. proposed the following formula to calculate a% [55]

$$a\% = 1 - \exp\left\{-\upsilon t_c \exp\left[\frac{-E_a}{kT_c + (1-e_r)M_a V_p^2/2}\right]\right\} \tag{5}$$

Where υ is the natural frequency of Eigen-oscillations of atoms in lattice, t_c is contact time, E_a is activation energy, T_c is contact temperature, k is Boltzman constant, e_r is recoil coefficient, M_a is the atomic mass and V_p is the velocity of the impacting particle.

$$Ad_{max}=S_c N_a E_1 \tag{6}$$

Where S_c is the contact area of a single particle to substrate, N_a is the total number of atoms in unit plane and E_1 is the energy of a single bond between two atoms.

Rebound energy is defined as the energy required to bounce the particle from the substrate during the unloading moment during deposition. Rebound energy (Re) is expressed as

$$R = \frac{1}{2} e_r m_p V_p^2 \tag{7}$$

Where m_p and V_p are mass and velocity of the particles and e_r is the recoil coefficient. Fig. 12 shows the calculated adhesion energy and rebound energy of three sizes (25 µm, 30 µm & 50 µm) of Al-Si particles at different velocity. The particle will only attach to the substrate when the adhesion energy is higher than the rebound energy. When the particle velocity is below the critical velocity and above the erosion velocity, the rebound energy is above the adhesion energy and no deposition can occur.

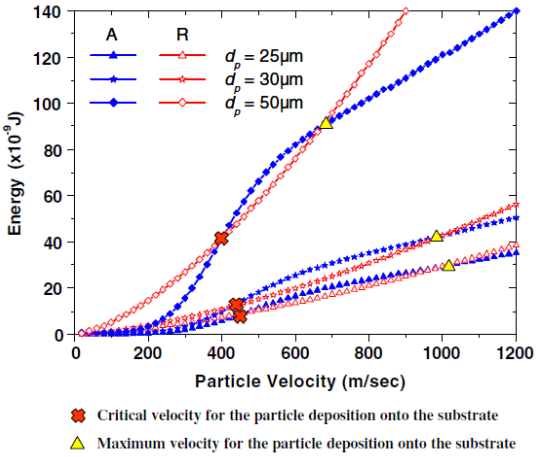

Fig. 12 Calculated adhesion energy and rebound energy for various sized Al-Si feedstock impacting onto mild steel [54]

3.2 Experimental investigations

A number of experimental studies to explore the particle-substrate interaction in cold spraying to understand the bonding phenomena have been reported [23, 30, 45, 46, 56-72]. This section summarizes the experimental findings on bonding behaviour in cold spraying and the factors which influence bonding.

3.2.1 Shear lips and craters formation

Early observations of particle-substrate interactions in cold spraying showed shear lips formation at the interface of deposited particles and crater formation of the substrate from the rebounded particles. Papyrin et al. [1] studied the interaction of individual aluminium particles with the copper substrate at different velocities to investigate the transition from rebound to adhesion of particles. At a lower particle velocity there were individual craters formed by the particle impact and there were no deposited particles. With increasing the particle velocity, particles started adhering to the substrate. These experiments showed that beyond a threshold velocity of the particles, critical velocity, a transition from substrate erosion to deposition occurs. The jet type morphology of shear lips around the deposited copper particles onto copper substrate was reported by Assadi et al. [7]. Hussain et al. studied the deformation behaviour of particles in copper-aluminium system [73] and titanium-steel system [71]. The deformation of the particles and substrates are related to their high strain rate material properties. Fig. 13 shows that the aluminium particles deposited onto copper substrate resulted in jetting of the particle, whereas copper particles deposited onto aluminium substrate caused jetting of the aluminium substrate. The jet type morphology was not noticed on the craters at the substrate left by non-adhering particles. Moreover, in a study of cold spraying of copper particle onto steel substrate, Dykhuizen et al. [61] reported that the crater formation is dependent on the particle velocity, i.e. with increasing the velocity the depth of the crater also increases.

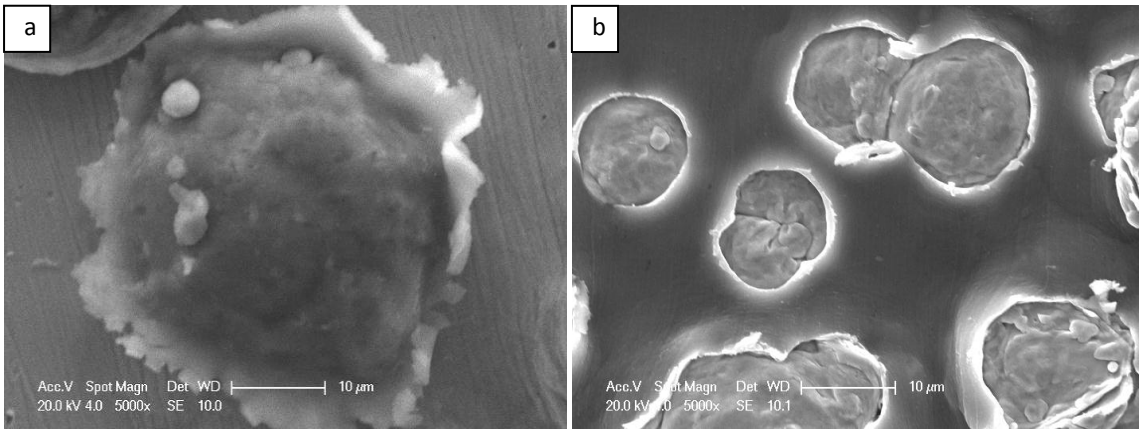

Fig. 13 Plan views of (a) Al particle on Cu substrate and (b) Cu particles on Al substrate [73].

3.2.2 Bonding in low pressure cold spraying

In low pressure cold spray system (LPCS) the particle velocity is well below the so called critical velocity for deposition. It is generally agreed that the metal particles must undergo severe plastic deformation to be deposited onto the substrate surface. In high pressure cold spray system, the velocity of the particle (above critical velocity) provides the required kinetic energy for this severe plastic deformation. Shear flow at the interface causes dissipation of kinetic energy which reduces the rebound flow and produces close surface connection. Plastic deformation following shear flow is dependent on a number of material properties and impact pressure. To facilitate shear flow upon impact, the material can be softened by thermal softening or the impact pressure can be increased by increasing the impact force or by reducing the contact area. At velocities below critical velocities the value of the impact force is insufficient to cause shear flow, hence the desired condition can be achieved by reducing the contact area. A rough surface with multiple peaks (in the powder scale) can result in extensive plastic deformation instead of a smooth surface.

It was first reported by Rocheville in 1963 [74] that using a supersonic nozzle at stagnation pressure of 1MPa resulted in powder adhering to the substrate by entering the pores of the surface where the particles was firmly retained thereon. A thin layer of few micrometers thickness formed on the surface, but no further buildup of coating upon itself was possible. This process is sometimes referred to as supersonic blasting. Low pressure cold spray systems utilise this concept for coating deposition.

To produce coatings using low pressure cold spraying system ceramic powder (e.g., alumina) is blended with the metallic powder. The main functions of the ceramic addition are the activation of the sprayed surfaces and hammering of the substrate/ sprayed layers by shot-peening [66, 75-77]. Ceramic particles in the feedstock result in compacting effect during the impact resulting in enhanced coating properties. Thick coatings can be deposited by increasing the small-scale roughness of the sprayed coating in this way. The random distribution of ceramic and metal particles in the spray plume results in random location of the impact points and results in coating build-up. Ceramic particles also contribute to cleaning of the nozzle of the gun. It was found that increasing the fraction of ceramic in the feedstock the bond strength and density of the coating increased. Supersonic blasting is restricted to the use of soft metal powders and rough substrates with low heat conductivity; the deposition process at low velocities is not adiabatic. This process is also termed as dynamic metallization (DYMET).

3.2.3 Removal of surface oxides

It has been proposed that the first layer of coating buildup (i.e., deposition of particles onto the substrate) involves, substrate surface cratering and activation of the surface by removing any surface contamination [1, 68, 69, 78]. Papyrin et al. argued that the first impinging particles increase the chemical activity of the surface by elevating the dislocation concentrations on the very top layer

[78]. During the particle deformation phenomena, the oxide shells on the interacting surfaces are broken and clean surfaces are pressed together and thus bonded. It has also been proposed that the interfacial material jet produced from adiabatic shear instability phenomena helps in removing the oxide films from the surface and thus enable an intimate metal-to-metal contact to be established [6, 7, 61, 69].

Kang et al. [62] and Li et al. [63] studied the role of oxide content of the powder on critical velocity for deposition. It was argued that the critical velocity of material does not only depend on material properties but also on oxidation condition. It was found that increasing the oxide content of the copper powder from 0.02 wt.% to 0.38 wt.%, the critical velocity increased from 300 m /s to 610 m /s [63]. In addition, Kang et al. [62] studied the role of oxide content of aluminium feedstock powder on critical velocity. It was reported that increasing the oxide content of the same powder size distribution from 0.001 wt.% to 0.045 wt.% increased the critical velocity from 742 m /s to 867 m /s. It was suggested that the critical velocity also depended on the oxide scale thickness. The thicker the oxide scale is, the more energy is required to remove the oxide and less plastic deformation energy is dissipated into the particle. Moreover, an increase in oxide content resulted in a decrease in particle flatting ratio. It is believed that the adiabatic shear instability at the particle-substrate interface can disrupt the oxide film; however, some part of the oxide remains at the interface which hinders particle-substrate adhesion [79]. Fig. 14 shows the presence of aluminium oxide at the interface of aluminium particle and substrate in a TEM image [62]. It was argued that the deformation of the particle was unable to remove the surface oxide layer. Price et al. [19, 65] also reported that the metal-to-metal bond had established in some regions of the coatings, whereas in other regions, metal-to-metal contact was inhibited by a thin layer of surface oxide film. By increasing the particle in-flight velocity, a greater degree of particle deformation was achieved, and hence a greater metal-to-metal contact between particles was established.

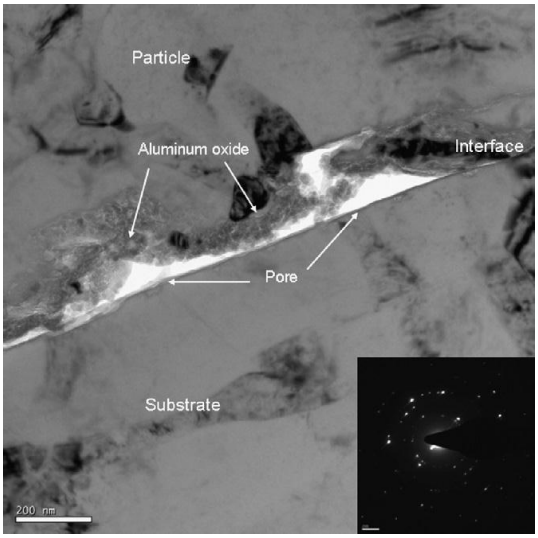

Fig. 14 FE-TEM micrographs: bright field image of interface between aluminium powder and substrate showing aluminium oxide layer [62]

In recent years, a number of TEM investigations of the interface of cold sprayed copper particles onto aluminium substrates have been published [46, 57, 58, 80]. In one study, it was argued that the bonding occurred between cold sprayed copper splats because of the two oxide films, which were on two separate particle surfaces, fused together to form one continuous layer. In addition, the particle surface could reach a very high temperature resulting in releasing of oxygen which could get trapped in the liquid film. At the copper particle-aluminium substrate interface a number of different phases including nano-crystallized phases and intermetallics were present within a thickness of ~20 nm, except the bottom of the splat. The authors argued that the thickness of the intermediate phases suggest that diffusion occurred in a liquid state than in a solid state [46, 57, 58].

It was hypothesized that transient melting might act as a mechanism in Cu-Al interaction. King et al. [80] also reported melting of aluminium substrate at the crater wall where the copper particle slid past aluminium. It was suggested that adhesion was promoted from the solid material jetting and molten material jetting, which also contributed to mechanical interlocking [46].

3.2.4 Contributions of mechanical and metallurgical components

A relatively new bonding model has been proposed in cold spraying which utilizes two mechanisms of bonding, namely that of metallurgical bonding between the coating and substrate and that of material extruded from the substrate during impact of the particles which is then interlocked within the coating structure (termed interlocked material) [72]. Fig. 15 shows such an example of interlocked material where aluminium was extruded in between copper particles and the fracture surface of the coating shows rim of aluminium around the copper particles. The contributions of these two mechanisms to the bond strength values were rationalized in terms of a modified composite theory. During bond strength testing, decohesion of the coating from the substrate must result in failure of both the metallurgically bonded regions and the mechanically interlocked material. It was reported that, mechanical interlocking was able to account for a large proportion of the total bond strength in cold sprayed copper coatings onto aluminium substrates, with metallurgical bonding only contributing significantly when the substrate had been softened prior to spraying.

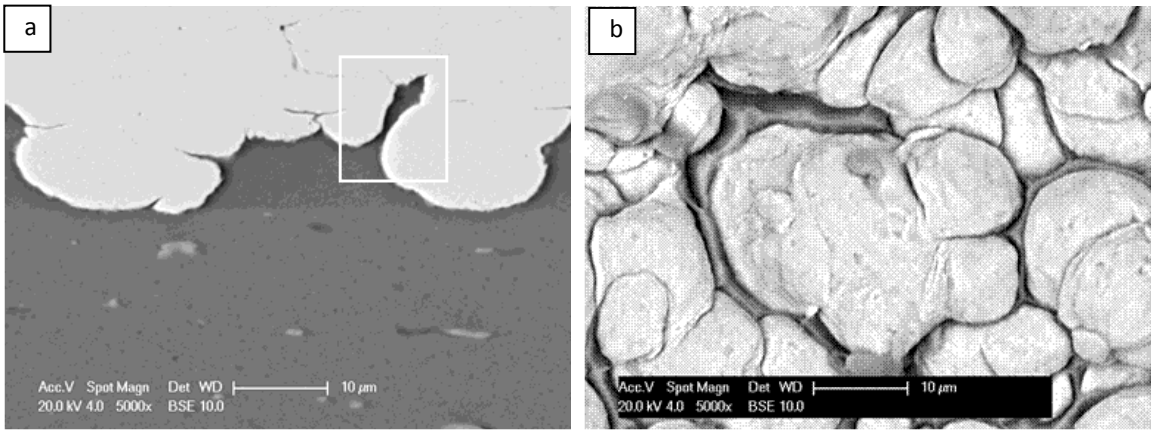

Fig. 15 (a) Copper coating on aluminium substrate showing aluminium extruded in between copper particles (b) Fracture surface (coating side) after pull off test on the same coating-substrate combination showing rim of aluminium around copper particles [72]

3.2.5 Interfacial curvature and instability phenomena

The nano-micro scale mechanical material mixing at the cold sprayed coating substrate interface was observed by several researchers [35, 50, 59, 81]. They attributed this mixing phenomenon to Kelvin- Helmholtz instability mechanism. In the Kelvin-Helmholtz instability phenomenon, when two fluids in contact are moving at different velocities parallel to each other, instability can occur (due to non-zero curvature of the interface) and one fluid flows around the other, a centrifugal force is generated. This centrifugal force might also promote amplification of the interfacial perturbation.

Champagne et al. [59] provided the following equation to estimate particle velocity required for interfacial material mixing

$$V_p = \left[(7.5\times10^4)\left(\frac{B'}{\rho_p}\right)\right]^{0.5} \quad (8)$$

Where V_p is the particle velocity, B' is the Brinell hardness number of the substrate and ρ_p is the density of the coating material. This equation shows that the interfacial material mixing depends on substrate hardness and coating material density. This interfacial material mixing may also be responsible for mechanical interlocking of the coating and substrate [50].

In addition, Klinkov et al.[50] proposed another mechanism called-"sticking" in bonding of cold sprayed material. In "sticking", the particle first sticks to the substrate due to Van Der Waals or electrostatic forces, and strong adhesion is only formed when incoming particles impact onto sticking particles. Van Der Waals is a very weak bond, which may contribute to the initial bonding but with subsequent impact the bonding is dominated by metallic bonding. Electrical conductivity measurements across the cold sprayed interfaces show high conductivity, which can only take place if there is metallic bonding (i.e., a bond with large number of free electrons).

3.2.6 Role of surface preparations

The bonding mechanisms operating in cold spraying of copper onto an aluminium alloy substrate was investigated experimentally as a function of different surface preparation procedures for the substrate, namely polished, ground and grit blasted substrate surface by Hussain et al [72]. Coating-substrate adhesion following spraying onto a grit-blasted surface was significantly reduced by grit embedment into the aluminium surface during blasting. It was suggested that grit-blasted surface restricted jet formation upon impact which resulted in less successful removal of oxide film from the interface and hence a weaker metallurgical bond. Marrocco et al. [82] explored the effect of different surface preparation techniques in controlling the bond strength of a cold sprayed titanium coating on Ti6Al4V. They proposed that grit-blasting of the Ti6Al4V substrate caused work hardening, which subsequently limited its deformation by impact of a titanium particle during cold spraying; it was argued that this restriction of substrate deformation led to lower bond strengths being observed. Wu et al. [83] studied an Al-Si coating, cold sprayed onto both polished and grit-blasted mild steel. Micro-pores and defects were found in the grit-blasted surface while an "intimate" interface was found following deposition onto a polished substrate; it was argued that the micro-pores on the grit-blasted surface resulted in lower bond strengths being observed. They also reported higher bond strength with increasing particle incident velocity. In contrast, Makinen et al. [84] found higher bond strengths for a copper deposit cold sprayed onto a grit-blasted copper surface compared to that observed for deposition onto an as-received surface.

The effect of substrate surface preparation on the deposition efficiency of the process has also been assessed. Sakaki et al. [85] reported a slight increase in the deposition efficiency of cold spraying of copper and titanium by increasing substrate surface roughness (grit-blasted substrate compared to polished substrate). Richer et al. [86] also reported an increase in deposition efficiency in spraying an aluminium alloy particle onto a coarser grit-blasted surface when compared to a finer grit-blasted surface. However, the substrate surface roughness has an effect only on the first few layers of coating deposited, and as such, the effect on deposition efficiency may be small, depending upon the significance of the coating initiation stage in the total time for coating development.

3.2.7 Coating build up mechanisms

Van Steenkiste et al. [69] studied the formation of cold sprayed aluminium coating with a relatively large powder particles (>50μm) and proposed a model to explain the coating build up process. The model was composed of four basic stages: in stage 1 the substrate surface is activated by substrate cratering and a first layer of coating is built up by fracturing the surface oxide layer, in stage 2 the particles deform and realign as a result of successive particle impact, in stage 3 metallic bond is formed which also results in a reduction of porosity and in the final stage the coating is further densified and work hardened. The four stages of coating build up is schematically shown in Fig. 16.

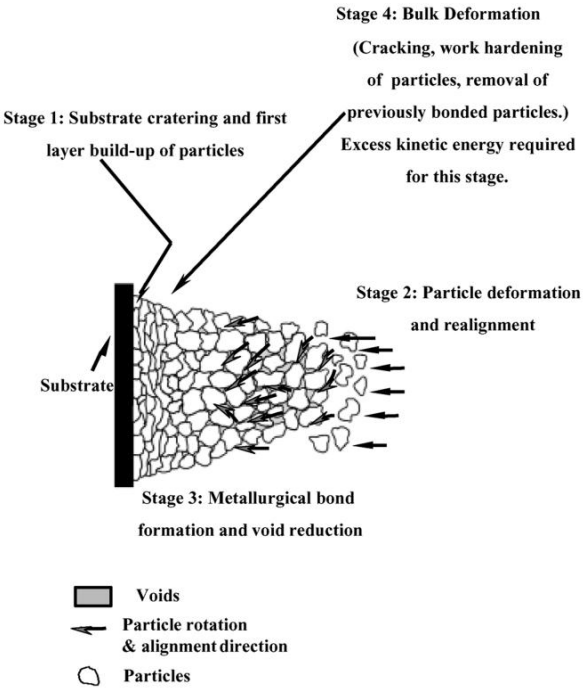

Fig. 16 Stages in coating formation in kinetic spray process [69]

3.3 Summary of bonding mechanisms

It is generally accepted that upon impact of a particle under certain conditions onto the substrate, the material goes through adiabatic shear instability phenomenon where thermal softening dominates over strain hardening and strain rate hardening and a material jet is produced. This material jet removes any surface oxide layer or contamination from the metal surface, so that freshly exposed metal surfaces come together to form a bond. A number of TEM studies have also showed evidence of ruptured oxide layer at the particle-substrate interface. In addition, adiabatic shear instability phenomenon to occur at the particle-substrate interface, the particle has to travel at a velocity higher than critical velocity and has a diameter larger than critical diameter. Moreover, there exists a window of particle velocities, within which deposition of particle can occur without erosion. It was also argued that bonding in cold spraying depends on a competition between plastic adhesion energy and elastic rebound energy. The bonding in cold spraying is thought to be a combination of (i) metallurgical bonding (ii) mechanical interlocking of the substrate material in the coating. The localized deformation and adiabatic shear instability play an important role in particle-substrate deformation. However, the actual mechanism by which this thermal softening and adiabatic heating promote bonding is not yet clear. Numerical simulations of particle impact in cold-spraying provide valuable information about the high stain rate deformation behaviour of materials, but are unable to provide a clear indication of the conditions under which intimate metallic bonding is established.

4 Cold spraying of titanium deposits

Cold spraying of copper and aluminium has been widely explored in the last decade, now it is of growing interest to the scientific and engineering communities to explore the potential of titanium and its alloys. Titanium as a barrier layer has a great potential for corrosion resistant applications and as a material for near net shaped manufacturing for the aerospace industry where reducing the machining cost is a key factor [87]. Moreover, titanium has found many applications due to its bio-inertness [88], i.e., titanium coatings can be used in the acetabular cup of a femoral component and vertebral prosthesis [89].

The potential difficulties in cold spraying of titanium are due to its high critical velocity, high reactivity with oxygen and crystal structure. The critical velocity of a 25 μm titanium particle is ~750 m/s, as calculated by numerical simulation, which is significantly higher compared to copper and aluminium [6]. Moreover, the high reactivity of titanium with oxygen at high temperature makes it challenging to spray titanium at higher process gas temperatures [90]. Furthermore, the hexagonal closed packed (hcp) crystal structure of titanium makes it difficult to deform the particles sufficiently to achieve a pore free coating [82].

4.1 Powder feedstock

Cold sprayed titanium deposits have been prepared from both angular feedstock powder and spherical feedstock powder [12, 82, 91-94]. Angular feedstock titanium powder is produced from hydride- dehydride process and spherical titanium powder is produced via inert gas atomization or plasma atomization process. In hydride-dehydride process, titanium is first hydrated by heating in a hydrogen atmosphere, the brittle titanium hydride compound is then easily crushed to desired size ranges which is then dehydried by heating in a vacuum [95]. In gas atomization process, a molten bath of titanium metal is levitated in a water cooled titanium shell (skull) to avoid contamination, and the molten metal flows through a nozzle which is then broken up using an inter gas into discrete particles. In plasma atomization process, there is no molten bath, titanium is fed in a wire form and plasma torches melt and atomize the powder in a vacuum [95-97]. The flowability of the spherical powder shows superior behaviour over angular titanium powder, which is desirable for uninterrupted powder feeding in various spraying process. However, the processing route for spherical titanium powder makes the end product quite expensive, i.e., a kilogram of spherical titanium powder with size ranges suitable for cold spraying is five times more expensive than that of angular powder.

4.2 Deposition efficiency and critical velocity

4.2.1 Deposition efficiency

Deposition efficiency of a material is calculated as a ratio of mass of bonded particles to the mass of the sprayed particles. Deposition efficiency of a material depends on process parameters and properties of the particle and substrate. Blose et al [98-100] reported that deposition efficiency of angular titanium powder with mean particle size of 21 μm onto titanium substrate is 85%, which means 85% weight of the sprayed particles deposited on the substrate. The deposit was prepared using helium as a propellant gas at 2.1-2.8 MPa and 400-500°C. Bae et al. [33] showed that an increase in particle velocity and temperature results in an increase in deposition efficiency of cold sprayed titanium onto mild steel. Increasing the particle velocity from 650 m/s to 950 m/s resulted in an increase in deposition efficiency from 85 % to 98 %. Moreover, increased particle temperature, using a powder preheating system, resulted in a higher deposition efficiency of titanium when the particle velocity was kept constant. Higher particle temperature could enhance the adiabatic shear instability zone and due to low thermal conductivity of titanium result in a higher plastic deformation zone. Wong et al. [12, 92, 93] reported a deposition efficiency up to 100% using both angular and spherical titanium powder sprayed onto mild steel substrate. It was reported that above an average velocity of 688 m /s the deposition efficiency reaches 100% [92, 93]. In cold spraying of spherical titanium powder (mean size 16 μm) onto Ti6AL4V deposition efficiency of ~100% was reported using heated nitrogen as propellant gas at 4 MPa and 800°C [101].

4.2.2 Critical velocity

Cold spray coating deposition is significantly influenced by the velocity of the particles and there exists a velocity called critical velocity, beyond which successful deposition can occur. A number of particle velocity measurement studies of titanium powders have been reported by several researchers [12, 93, 102-104]**.** In the particle image measurement technique, velocity is measured

by determining particle displacement over a short period of time using pulsed laser. Several methods exist in the ways critical velocities are measured. In numerical modelling, critical velocity is the velocity at which adiabatic shear instability occurs. In particle velocity measurements, critical velocity is the velocity when the transition from erosion to deposition occurs. Critical velocity can also be estimated from a knowledge of deposition efficiency, particle velocity and particle size distribution. Marrocco et al. [82] estimated the critical velocity by this method to be ~690 m/s for angular titanium powder. Schmidt et al. [6] numerically modelled the particle impact deformation behaviour using a finite element model and reported a critical velocity of around 750 m/s for a 25 μm titanium particle. Wong et al. [93] measured the critical velocity of spherical titanium powder (mean diameter 29 μm) using particle image velocimetry to be between 505 -610 m /s. It was also reported that a higher particle temperature leads to a lower critical velocity of titanium due to thermal softening of the particles.

4.2.3 Effect of particle velocity and temperature

Particle velocity and temperature are the two most important factors in deposit formation. Beyond the limit of critical velocity, a further increase in particle velocity results in a decrease in deposit porosity. A recent study using optimized process parameters and nozzle design achieved an average velocity of 1173 m/s using helium as an accelerant gas [12]. As a result of this high velocity, the deposit produced was less porous. It was also reported that an increase in particle velocity results in a smoother deposit surface due to better packing and contact between splats [105]. In wipe tests of spherical titanium particles onto titanium substrates, it was seen that with increasing particle velocity and temperature, the degree of splat formation and jetting was increased [104].

The morphology of the powder also influences the velocity of the particles in the gas stream. It was observed that the velocity of angular titanium particle was always higher than the velocity of spherical titanium particles for the exact same conditions. It was argued that the drag coefficient of angular powder is higher than spherical powder with the same mass, hence acceleration for angular powder is higher [92].

Zahiri et al. [103, 106] measured the velocity distribution of the supersonic plume at various process gas pressures and temperatures. An increase in the process gas temperature contributed to an acceleration of in-flight particles at the vicinity of nozzle exit. However, an increase in process gas pressure expanded the region of the high velocity particles within the gas stream outside the nozzle. The particles at the centre of the nozzle had a higher particle velocity compared to the particles at the edge showing a bell shaped particle distribution. Moreover, it was reported that using helium as an accelerant gas significantly increases the high velocity plume outside the nozzle compared to heated nitrogen gas as an accelerant.

4.3 Bond strength

Bond strength values of cold sprayed commercially pure titanium deposits onto mild steel and Ti6Al4V alloy substrates have been reported by several researchers [33, 82, 101, 107-109]. The bond strength tests of the deposits were normally carried out according to the ASTM C633 standard. The deposit was glued to a counterpart using thermal curing epoxy and then pulled apart. A low bond strength value of cold sprayed titanium deposit onto mild steel substrate has typically been reported in the literature (i.e., ~20 MPa). This should be compared with typical HVOF sprayed WC-Co coating where pull-off strength is >80 Mpa. However, improvement of cold spraying apparatus, gun design and optimizing process conditions has resulted in an increase in bond strength values. Bond strength value of cold sprayed coating is a function of particle velocity and hence plastic deformation upon impact. A recent study by Bae et al. [33] reported a bond strength value of at least as high as 85 MPa (strength of the epoxy was 85 MPa) for cold sprayed titanium coating onto mild steel substrate. A commercially available CGT Kinetics cold spray system with helium as a propellant gas was used to reach a particle velocity of 950 m/s. It should also be noted that the surface of the mild steel substrate was prepared in a grit blasted finish with a coarse grit (350 μm)

which also contributed to mechanical interlocking of the coating with the substrate. Wong et al. [92] also reported that grit blasting of mild steel with size 24 (~764 μm) alumina as a method of surface preparation produced strong bonding with a titanium deposit. However, Marrocco et al. [82] and Price et al. [109] both reported a decrease in bond strength values of cold sprayed titanium coatings when the substrate was grit blasted. It was argued that the work hardening phenomena associated with grit blasting might have made it difficult for the sprayed particle to bond to the substrate.

Table 1 Pull-off bond strength values of Ti coatings

References	Bond strength [MPa]	Substrate	Substrate preparation	Gas pressure, temperature & powder type	Equipment
Wang et al. [107]	8-16	Mild steel	Grit blasted (24 mesh alumina)	350-650°C N_2 at 2 MPa, 500°C air at 1.5-2.0 MPa, angular Ti	Xi'an Jiaotong University
Li et al. [108]	15 ± 4	Mild steel	Grit blasted	520°C air at 2.8 MPa, angular Ti	CGT/ LERMPS
Bae et al. [33]	50[a] 65[b] >85[c]	Mild Steel	Grit blasted (350 μm alumina)	600°C N_2 at 2.5 MPa (with[a]/without[b] preheating), 600°C He at 1.5 MPa[c], spherical Ti	CGT 3000
Marrocco et al. [82]	23[d] 22[e] 7[f]	Ti6Al4V	Polished[d], ground[e] & grit blasted[f]	Room temp He, angular Ti	University of Nottingham
Price et al. [109]	37[g] 32[h]	Ti6Al4V	As received[g], grit blasted[h]	Room temperature He, angular Ti	University of Nottingham
Hussain et al. [101]	71 ± 6[i] 57 ± 8[j] 64 ± 27[k]	Carbon Steel[i] Stainless Steel (304)[j] Ti6Al4V[k]	In-situ grit blasting of steels and as received Ti6Al4V	800°C N_2 at 4 MPa, spherical Ti	CGT 4000

A new method; a modified ball bond shear test method, to measure the adhesion strength of the cold sprayed splats has been recently reported by Chromik et al.[104] . The adhesion strengths of titanium splats onto bulk titanium substrate was observed on the order of 240 MPa, which is approximately 63% of the bulk shear strength of titanium, for velocities above 770 m/s. However, it is not clear how this relates to traditional pull-off test values.

4.4 Porosity of the deposits

Porosity in cold sprayed titanium deposit depends on a number of factors, such as particle velocity and particle temperature hence particle deformation. Therefore, minimization of porosity can be achieved by process parameter optimization. Table 2 shows the volume fraction of porosity values reported in literature. Compared to cold sprayed materials like copper, nickel and aluminium,

titanium typically shows a higher degree of porosity. The porosity of cold sprayed titanium deposits varied from 20- 0.1% depending on process conditions. Earlier investigations in cold spraying of titanium using coarser angular powder and customized spraying systems resulted in a porosity level of around ~20% [82]. Modern cold spraying equipment is reportedly capable of producing cold spray coating with 0.1% porosity using heated nitrogen or helium gas. It is generally agreed that the critical velocity of titanium powder is around 700 m /s. It is noticed that increasing the velocity of the particle by increasing gas temperature and pressure results in a lower porosity coating, as can be seen from Table 2 [12, 92-94, 102]. Higher particle velocity also gives reduced porosity. In addition, Zahiri et al. [110] reported a deposit porosity of 0.5 % by increasing the particle velocity to 1380 m/s. In general, the porosity decreased further when the particle velocity was increased using helium as accelerant gas. However, the role of particle morphology in cold sprayed titanium deposit is not yet clear. Porosity of less than 1% has been achieved both from hydride de-hydride angular powder and gas atomized spherical powder. Although, it is hypothesised that the angular shape of the particle might be beneficial in getting rid of interparticle pores through plastic deformation [92], the experimental results are still not conclusive.

Temperature of the impacting powder particle also contributes significantly in reducing the porosity. Bae et al. [33] reported a decrease in porosity from 9.5% to 1% by preheating the powder to 600 °C, thus enhancing thermal softening. In addition, Zahiri et al.[110] reported that with increasing the standoff distance in cold spraying the volume fraction of porosity increases. This is due to a longer travelling distance outside the nozzle which leads to a deceleration of particles. Moreover, a small particle size and narrow particle size distribution was reported to lead to reduced porosity, for example using a mean particle diameter of 16 μm instead of 22 μm led to a decrease in porosity value by 1.5%. Furthermore, X-ray microscopy and microtomography was utilized to visualize the pores in cold sprayed titanium deposit [111].

Porosity measurements on cross-section images from optical microscope and scanning electron microscope are sensitive to sample preparation. Smearing of titanium coating surface could occur if special care is not taken. In imaging techniques, a 2D representation of the surface of the sample with some contrast mechanism is used to distinguish pores. Moreover, in an ideally prepared sample surface the measurement of porosity is limited by the resolution limit of the microscope [112]. Furthermore, automated image analysis requires careful selection of pore boundaries. Mercury intrusion porosimetry (MIP) was used by Hussain et al. [113] to characterise the interconnected porosity over a size range of micrometers to nanometers of free standing titanium deposits. The results showed that a significant proportion of the porosity was sub-micron and so could not be reliably measured by optical microscope based image analysis.

Table 2 Porosity of cold sprayed titanium coatings reported in literature

Ref.	Porosity	Porosity measurement technique	Gas pressure, temperature & powder type	Equipment	Notes
Marrocco et al. [82]	~20 %	Image analysis of optical method	2.9 MPa He at room temperature with angular powder	University Nottingham	Particle velocity 690 m/s (numerical model)
Zahiri et al. [110]	9.5 %[a] 0.5[b] %	Water displacement ASTM C 20: 2000	2.4 MPa N_2[a] & 1.5 MPa He[b] at 600 °C with angular powder	CGT 3000	720 m/s & 1380 m/s
Wong et al. [12, 92, 93]	20 %[c] 2%[d]	Image analysis	3 MPa at 300 °C[c] & 4 MPa at 800°C[d] N_2 with spherical powder	CGT 4000	610 m/s & 805 m/s
Bae et al. [33]	9.5 %[e] 0.1 %[f]	Image analysis	2.5 MPa N_2[e] and 1.5 MPa He[f] at 600°C with spherical powder	CGT 3000	650 m/s & 950 m/s
Gulizia et al. [94]	11 %[g] 1 %[h]	Image analysis	2 MPa at 400°C[g] & 3.5 MPa at 800°C[h] N_2 with spherical powder	CGT 4000	
Chromik et al.[104]	1.6 %[i] 1.0 %[j]	Image analysis (LOM)	3 MPa at 500°C[i] & 4 MPa at 800°C[j] N_2 with spherical powder	CGT 4000	695 m/s & 825 m/s
Hussain et al. [101, 113]	11.3 %[k] 5.9 %[l]	Mercury intrusion porosimetry (MIP)	4 MPa at 600°C[k] & 800°C[l] N_2 with spherical powder	CGT 4000	

4.5 Microhardness of the deposits

Table 3 shows the average hardness values of cold sprayed titanium deposits reported by various researchers. The measurement of microhardness on sprayed deposits like titanium is challenging due to the presence of porosity. The porosity in the deposits can contribute to a lower microhardness value and scattering of the data; therefore, microhardness values should be interpreted carefully. Typical microhardness of a commercially pure grade 1 bulk titanium is ~145 kgf/ mm^2 and that of a gas atomized spherical titanium powder is ~141 kgf/ mm^2 [92]. Increasing the process gas temperature leads to an increase in microhardness because of increased particle acceleration and exit velocity. Higher process gas temperature increases the speed of sound in the process gas and so the particle velocity is increased. Increasing the process gas temperature can also contribute to thermal softening of the powder. It was generally found that an increase in particle velocity results in an increase in deposit hardness [102]. A higher particle velocity will lead to greater amount of bonding between splats, compaction within the splats and higher dislocation density. It was found that microhardness at the bottom of the deposit was always greater than the

top of the deposit in cold sprayed titanium. This was attributed to a greater degree of deformation of the particles at the bottom layer [101]. Higher deformation results in work hardening which may be related to twinning, dislocation pile ups and imperfections during deformation.

Gulizia et al. [94] reported an average increase of hardness of cold sprayed titanium deposit by 16% compared to bulk materials. However, in cold spraying of copper and aluminium, an increase of 50% to 100% in hardness was reported [94]. The hexagonal closed packed (hcp) structure of titanium makes it more resistant to deformation. An increase in hardness values compared to the bulk of any material can be attributed to fine grain structure and/ or a high dislocation density.

Moreover, nanoindentation hardness measurements on cold sprayed titanium deposits, prepared from angular feed stock, was carried out by Moy et al. [114]. Nanoindentation tests showed occasional lower values due to imperfections or porosity within the titanium deposit with a typical microhardness value of 350- 460 kgf /mm^2. Nanoindentation hardness measurements are confined to small area of the deposits, which makes it challenging to compare with the bulk microhardness values reported in literature.

Table 3 Hardness of titanium deposits reported in the literature

Ref.	Vickers microhardness [kgf /mm^2]	Gas pressure, temperature & powder type	Equipment	Notes
Zahiri et al. [110]	150[a] 320[b]	2.4 MPa N_2[a] & 1.5 MPa He[b] at 600 °C with angular powder	CGT 3000	Particle velocity 720 m/s & 1380 m/s
Zahiri et al. [115]	320	1.5 MPa He at 600 °C with angular powder	CGT 3000	Measured on ground cross section
Wong et al. [12, 92, 93]	190[c] 220[d]	3 MPa at 300 °C[c] & 4 MPa at 800 °C[d] N_2 with spherical powder	CGT 4000	Powder hardness 141 kgf/ mm^2
Bae et al. [33]	180[e] 260[f]	2.5 MPa N_2[e] & 1.5 MPa He[f] at 600 °C with spherical powder	CGT 3000	-
Gulizia et al. [94]	275[g] 300[h]	2.0 MPa at 400 °C[g] & 3.5 MPa at 600 °C[h] N_2 with spherical powder	CGT 4000	Powder hardness 244 kgf/ mm^2 and indentation load 5g
Hussain et al. [101]	217 ± 12[i] 281 ± 2[j]	4.0 MPa at 600°C[i] & 800 °C N_2[j] with spherical powder	CGT 4000	Indentation load 100 gf

4.6 Constituents of cold sprayed titanium

4.6.1 Composition: oxygen nitrogen levels

The oxygen and nitrogen contents of the commercially pure titanium powder and titanium deposit prepared using cold spraying have been reported by Li et al. [90, 116], Gulizia et al. [117] and Hussain et al. [101]. Table 4 shows the measurements of oxygen and nitrogen in starting feedstock

powder and in the deposits. Nitrogen and oxygen levels increased in cold sprayed deposits compared to the starting powder. However, the oxygen and nitrogen contents of the deposits are well below the level of any thermal sprayed titanium deposits. It was also reported that [117] an increase in oxygen content occurs with increasing the process gas temperature of the cold spraying. The increase in process gas temperature results in an increase in particle temperature and hence, higher tendency to oxidation.

Table 4 Oxygen-nitrogen contents of titanium powder and cold sprayed deposits

Ref.	Powder		Deposit		Gas pressure, temperature & powder type	Equipment
	O (wt.%)	N (wt.%)	O (wt.%)	N (wt.%)		
Li et al. [90, 116]	0.31	0.07	0.6	0.1	520°C air at 2.8 MPa, angular powder	LERMPS/CGT
Gulizia et al. [117]	0.437	0.011	0.517	0.026	3.4 MPa N_2 at 400°C angular powder	CGT 4000
			0.539	0.024	600°C	
			0.588	0.035	800 °C	
Hussain et al. [101]	0.14	0.01	0.34	0.03	4.0 MPa N_2 at 800° C, spherical powder	CGT 4000

4.6.2 Microstructural features

Cold sprayed titanium deposits show two distinctive regions: a porous top layer and a less porous bottom layer. Deposits prepared from both angular powder and spherical powder resulted in these two distinct regions of porosity [82, 91, 92]. It was observed that the size of the pores reduced towards the bottom of the deposit. Moreover, the deformation of the particles and the flattening ratio were also increased towards the interface [114]. The tamping effect on the particles at the bottom layer by successive impacts of the following particles resulted in this less porous microstructure at the bottom. During the spraying of titanium, a flashing jet outside the nozzle was observed which is thought to be due to the reaction with oxygen in the air [90]. It was argued that the oxide layer on the surface of titanium powder is broken up due to friction and the porous structure of the deposits was attributed to this surface activity during spraying [116].

Transmission electron microscopy (TEM) was used to investigate the interparticle microstructure of the deposits and deposit-substrate interface [114, 118]. The interface of the titanium deposit onto aluminium substrate showed a sharp interface, indicating both deposit and substrate remained solid during impact and hence a metal-to-metal bond was established [114]. Although a number of other TEM studies reported formation of intermetallics in cold spraying of copper, aluminium and nickel, no such phenomena were noticed in titanium. It was argued that the high melting point of titanium makes it difficult to form secondary phase along the interface. Bae et al. [119] observed two regions in titanium deposit: a region of larger grains (>250nm) with high dislocation density and a region of smaller nanocrystalline grains (<100nm) with dislocation free grain boundaries. The authors argued that the dislocation free grains were mostly attributed to the relatively high temperature generated during strain accumulation, due to successive impact of particles, along with low thermal conductivity of titanium [119]. It was also believed that thermally activated static recovery process contributed in annealing out of dislocations in the smaller grains. The high density dislocations in the grains can provide strain hardening and increased ductility of the material. Also, the fine grained nano structure can promote grain boundary sliding and consequently enhance ductility.

Metal-to-metal bond formation within the titanium deposit was reported in literature in etched titanium deposit [90, 108]. Probably, the high particle surface temperature during the impact contributed to this scenario. It is also debated in the literature that the local surface melting of titanium can occur due to low thermal conductivity and resulting thermal diffusivity of titanium [33, 108]. Titanium also has a higher adiabacity compared to copper, aluminium and nickel for the same particle size range and velocity. Adiabacity is defined as the level of localized thermal build up during the high strain rate deformation process [33]. Moreover, Bae et al. [33] reported nano sized, spheroidical particles on the deposit surface when titanium was sprayed using helium as an accelerant gas at 950 m/s particle velocity. These small spherical particles were thought to be a sign of melting which was also supported by numerical simulations.

Microstrain measurements using Williamson-Hall method [120] of peak broadening of using X-ray diffraction were performed on commercially pure titanium particle and cold sprayed deposits [114, 121]. Table 5 shows the microstrain of titanium powder and the cold sprayed deposit prepared from that powder. Rafaja et al. [121] reported an increase in microstrain from 6.4×10^{-4} to 2.2×10^{-3} following cold spraying. The increase in microstrain in the deposit is due to severe plastic deformation of the powder during the deposition process. It was also reported that a steep increase in microstrain in titanium deposits occur from the top of the deposit to the interface [121]. This suggests that the titanium is mostly deformed at the particle-substrate interface. In addition, Hussain et al. [101] reported an increase in microstrain of the deposit when the process gas temperature was increased which resulted in a greater particle deformation evidenced in the microstructural investigations.

Table 5 Microstrain determination of Ti powder and deposits

Ref.	Microstrain in powder	Microstrain in deposit	Gas pressure, temperature & powder type	Equipment
Rafaja et al. [121]	6.4×10^{-4}	2.2×10^{-3}	2.5 MPa N_2 at 450°C, angular powder	CGT
Moy et al. [114]	7.0×10^{-4}	4.5×10^{-3}	1.5 MPa He at 600°C, angular powder	CGT 3000
Hussain et al. [101]	-	2.9×10^{-3}	4.0 MPa N_2 at 600°C, spherical powder	CGT 4000
		3.6×10^{-3}	at 800°C	

X-ray photoelectron spectroscopy (XPS) is a technique that measures the elemental composition of the material [122]. In XPS, a beam of X-rays with fixed wavelength are focused on the surface and photoelectrons are released from the atoms at the top few nanometres on the material surface. The kinetic energy of the released electrons can be related to the binding energy of the electrons in the atoms. Moy et al. [114] and Gulizia et al. [117] investigated the surface of cold sprayed titanium deposits using XPS. Gulizia et al. [117] reported a complex structure of several phases, i.e., titanium metal, titanium nitrides, oxides and oxi-nitrides in a range of stoichiometries on the deposit surface. Moy et al. [114] argued that nitrogen was picked up during the spray in form of N and TiN. Also, the amount of N shows a slight increase closer to the interface. Gulizia et al. [117] reported that an increase in Ti 2p signal associated with lower oxidation states occurs with increasing process gas temperature. The high reactivity of titanium with nitrogen and the occurrence of flashing jet during the deposition of titanium were thought to be responsible for this phenomenon [108]. However, when XRD was used, TiO or TiO_2 was not found in cold sprayed titanium deposits within the detectable range of XRD [116, 121].

4.6.3 Residual stresses

Residual stress in cold sprayed deposit is usually compressive in nature and tensile in the substrate, unlike thermal sprayed deposits where tensile residual stresses form in the deposits due to solidification of the splats. The tensile residual stress has a detrimental effect on fatigue endurance limit of the material. Residual stress of titanium deposits produced by cold spraying were investigated by Gulizia et al. [94] and Price et al. [109]. The layer by layer mechanical removal for measurement of residual stresses is challenging because the mechanical removal process of material can itself introduce stresses in the deposits. It is also possible to measure by profilometry the radius of curvature of the beam samples caused by application of the coatings, which can be used with Young's moduli to calculate residual stresses.

Increasing the process gas temperature and pressure results in an increase in residual stress within the titanium deposit. Compressive residual stress as high as 3.5 MPa, measured using XRD, was reported using process gas temperature of 800 °C at 3.5 MPa. Residual stress in cold sprayed titanium deposit is higher than cold sprayed ductile materials, like aluminium, due to different crystal lattice structures. The yield stress of titanium is relatively high which contributes to a high level of stress by simply following the stress strain curve during plastic deformation. This can contribute to the high residual stresses found in the deposits. Also, the high melting point of titanium means it is more difficult to relax the residual stresses.

4.7 Mechanical properties of deposits

Cold spraying has a high potential to build up ultra thick deposits and net shaped manufacturing product for rapid prototyping for automotive and aerospace industry. Machining high strength materials i.e., titanium is difficult and time intensive so there is a great interest in producing thick titanium deposit with desirable mechanical properties. Typical tensile stress-strain relationship of titanium deposit produced from angular powder feedstock is available in literature. Blose et al. [98] reported that the tensile strength of the as-sprayed titanium deposit was 100 MPa and the as sprayed deposit showed limited ductility due to interparticle defect and porosity. However, Zahiri et al. [115] used a commercially available cold spray system with higher pressure of helium gas and reported a tensile strength of 800 MPa for as-sprayed deposit, which was higher than that of commercially pure bulk titanium. A significant reduction in porosity of the deposit contributed to this high tensile strength value. However, the ductility of the as-sprayed deposit was limited to plastic deformation of 0.02%. Moreover, this ductility of the as sprayed material was improved following annealing.

The elastic modulus of the cold sprayed titanium deposit was measured by various techniques (i.e. knoop indentation, four point bending and nanoindentation) [19, 105, 114]. Young's modulus of titanium deposit using indentation and four point bending tests were ~20 GPa, which is significantly lower than the young's modulus of a bulk material which is 120 GPa. Limited bonding between interparticle splats due to porosity resulted in the lower Young's modulus. In addition, a recent study by Moy et al. [114] reported a Young's modulus of the titanium deposit between 92 GPa and 120 GPa measured using nanoindentation technique. It is important to mention here that bulk bending test samples a large number of particles and interfaces, so the modulus is sensitive to defects such as oxide inclusions and to inter-particle porosity. In the case of nanoindentation, individual particles are sampled, so the measured elastic modulus can be close to the bulk value as the contribution from oxides and porosities is reduced.

Tubular coating tensile (TCT) test is a fast and cost-efficient way of providing tensile strength of the deposits [5, 123]. The ultimate tensile strength of the TCT samples prepared from commercially pure titanium feedstock showed an increase in strength with reducing porosity. It was reported that when the porosity of the titanium deposit increased from 0.13 to 1%, the tensile strength of the deposit reduced to half. In addition, the tensile strength of the deposit increased linearly with increasing process gas temperature; the tensile strength of titanium deposit reached a value of ~450 MPa at a pressure of 4.0 MPa and 1000 °C using nitrogen as an accelerant. Hussain et al. [101]

reported a mean ultimate tensile strength of 247 ± 15 MPa for titanium deposit which was sprayed with commercially available CGT system using nitrogen at 800°C at 4.0 MPa. The tubular coating tensile strength data was verified using micro flat tensile (MFT) test. In MFT test, tensile test samples are produced using electro discharge machining and typical stress-strain properties are investigated under one dimensional condition. It was shown that the TCT tensile strength values correlated in a linear way with the MFT tensile strength values.

4.8 Effect of heat treatment on deposits

Post deposition heat treatment is used to reduce porosity and internal defects and to improve mechanical properties of the sprayed titanium and titanium alloys [124]. A number of post spray techniques to alter the microstructure and hence to optimize the cold sprayed titanium deposit have been reported in literature [98, 99, 113, 115, 116, 125, 126]. Zahiri et al. [115] reported that annealing at 350-550 °C resulted in ultrafine grains (<5 μm) formation in 25% of the area with an average grain size of 7μm. The ultrafine grains provide the mechanical strength to the deposits and larger grains provide the ductility to the material. In addition, annealing of cold sprayed titanium resulted in an elongation of 8%, which was a significant improvement in the ductility compared to the as-sprayed condition. However, the strength of the material decreased from 800 MPa to 600 MPa following annealing.

Heat treatment of titanium deposits results in recovery, recrystallization and grain growth, although it was difficult to identify the recovery stage in the isothermal annealing experiments [115]. Annealing of cold sprayed titanium deposit resulted in metallurgical bond formation and removal of particle-particle interface due to recrystallization and grain growth [116]. It was also noticed that micro-pores are generated in the annealing process in the healing of the interface through atom diffusion. Fracture surface analysis of the annealing deposit showed evidence of ductile failure.

Vacuum heat treatment to reduce porosity levels below the as-sprayed condition was used by Hussain et al [113]. Heat treatment of free standing titanium deposits significantly reduced the interconnected porosity; pores above 1 μm were reduced to 0.2 vol.% from 1.4% and pores below 1 μm were reduced to 1.6 vol.% from 4.6 vol.%. Laser surface melting of cold sprayed titanium deposits to eliminate interconnected porosity from the top layer was investigated by Marrrocco et al. [126]. It was reported that laser surface treatment was successful in eliminating any interconnected porosity from top ~140 μm without any delirious effect on the substrate. In addition, laser treated titanium deposit behaved similar to a piece of bulk titanium in salt solution.

Blose et al. [98, 99] also studied the properties of cold sprayed titanium and titanium alloys with post spray heat treatment and hot isostatic pressing (HIP). Heat treatment at 840 °C for four hours of commercially pure titanium deposits, which was prepared from angular powder, improved in yield strength and ultimate tensile strength by a factor of 2.5 but the elongation to failure was still very low (<1%). However, HIPing resulted in an increase in yield strength and ultimate tensile strength by a factor of 3.5 over the heat treated sample and elongation of the sample increased to 4%. Moreover, after HIPing the porosity of the deposits was reduced to zero.

4.9 Cold sprayed vs. warm sprayed titanium

Warm spraying is a modified form of high velocity oxy-fuel (HVOF) spraying technique in which nitrogen gas is mixed with the HVOF flame jet to lower the temperature of the powder particles [127]. A number of studies of high strain rate deformation behaviour of warm sprayed titanium have been published recently [127-134]. During warm spraying, titanium powders are heated to approximately half of the melting temperature. Oxidation of the particles occurs during the flight due to high temperature. The oxygen level in the warm sprayed titanium deposits sprayed using optimized parameters were ~1.5 wt.%, which was produced from a powder with 0.14 wt.% oxygen content [135]. The oxygen content of the warm sprayed titanium deposits is 2.5- 3% higher than

cold sprayed titanium deposits reported in the literature. However, the particles had very high deposition efficiency and bonded well due to thermal softening. In addition, fully nanocrystalline particles were formed by dynamic recrystallization [130]. Moreover, the warm spraying is reportedly capable of producing titanium deposits with porosity levels less than 1%.

4.10 Summary of cold sprayed titanium

A summary of the literature on cold sprayed titanium deposits is as follows:

- Typical deposition efficiency of titanium particles is 85– 100 % for both angular and spherical powder. The flowability of the spherical titanium powder shows superior behaviour over angular titanium powder.
- Titanium has a higher so called "critical velocity" of deposition. Typical critical velocity for deposition of titanium particle is considered to be in the range of 500- 750 m/s.
- Typical bond strength values of ~50-85 MPa are achieved using the state of the art high pressure cold spraying systems on steels and titanium alloys. It has been found that the grit blasting using coarser alumina improved the bond strength value.
- Cold sprayed titanium deposit contains relatively high porosity compared to other cold sprayed deposits (e.g., copper). Porosity values of the deposits range from ~ 10 to 1% when optimised process parameters were used. However, the porosity values are subjected to the limitations of the measurement techniques.
- The microstructure of a cold sprayed titanium deposit typically shows a porous top layer and a less porous layer closer to the deposit-substrate interface. The impact and compaction of the cold sprayed particles result in this less porous layer beneath the surface.
- The microhardness of the titanium deposits is higher than that of the bulk material. Typical values of the coatings are in the range of 150 to 300 kgf/ mm^2. However, the presence of porosity in the deposits can contribute to significant variations in microhardness.
- Both oxygen and nitrogen levels in the deposits show an increase following deposition in comparison with feedstock powder. Typical values of oxygen content in the coatings are ~0.3- 0.6 wt. %, when prepared from powders containing 0.1- 0.4 wt. % oxygen. However, the oxygen contents in the cold sprayed titanium coatings are three times lower than that of warm sprayed titanium coatings.
- Tensile strength of the titanium deposits shows a wide range of values from 100 to 800 MPa depending on the porosity level. However, the elongation to failure for all the deposits is very small. In addition, a new method termed the tubular coating tensile test (TCT) is used to measure the tensile strength of titanium deposits (typical value of 450 MPa), which correlates well with the microflat tensile tests. Young's modulus of the titanium deposits (20 MPa) is significantly lower than the Young's modulus of the bulk material (100 GPa) because of limited bonding between particles and porosity.
- Hot isostaic pressing (HIP) and vaccum heat treatment of titanium deposits can increase the tensile strength by three times and reduce the level of porosity to ~1%. Post deposition laser surface melting of titanium deposits can eliminate any interconnected porosity from top ~140 μm, without any delirious effect on the substrate, which performs similar to a piece of bulk titanium in salt solution.

5 Concluding remarks

Cold spraying is a rapidly developing surfacing and near-net shaped metal deposition technique with a wide range of applications. Commercially available state of the art cold spraying apparatus is making it possible to deposit a number of challenging materials. A number of research projects have

studied the bonding mechanisms in cold spraying; however, the mechanism of bonding in cold spraying is still a matter of some debate. A clear understanding of the bonding mechanisms will not only provide a useful ground to develop coatings with better properties but will also allow exploration of the difficult to spray materials.

Deposition of titanium using the cold spraying technology is considered a niche area. There is a considerable interest in developing titanium deposits as barrier layers for corrosion applications and near-net shaped metal deposition. Thick titanium deposits (several millimeters) can be produced with the state of the art cold spraying technology; although, it is still difficult to achieve a pore-free microstructure. The mechanical properties of the cold-sprayed titanium deposits are critical for commercial applications. Post-spray treatments can be used to eliminate porosity from the cold-sprayed deposits. It is greatly anticipated that with the progress in nozzle design, optimized powder production and developments in spraying apparatus, a pore-free titanium deposit may be achievable in the coming decade.

6 Acknowledgement

At the time the work was carried out the author was a doctoral researcher in the Division of Materials, Mechanics and Structures, Faculty of Engineering, University of Nottingham, UK. The author acknowledges financial and technical support from TWI Ltd. (Cambridge, UK) and an Overseas Research Studentship (ORS) from the University of Nottingham (Nottingham, UK). The author is also grateful to Prof D G McCartney and Prof P H Shipway from the University of Nottingham and Dr T Marrocco from TWI for many useful discussions on this review subject.

7 References

[1].Papyrin, A.N., *Cold spray technology* 2007: Elsevier.

[2].Davis, J.R., *Handbook of thermal spray technology*2004: TSS/ASM International.

[3].McCune, R.C., Hall, J.N., Papyrin, A.N., Riggs II, W.L., and Zajchowski, P.H., *An Exploration of the Cold Gas-Dynamic Spray Method for Several Materials System*, in *Advances in Thermal Spray Science and Technology*, C.C. Berndt and S. Sampath, Editors. 1995, ASM International: Houston, TX. p. 1-5.

[4].Grujicic, M., Zhao, C.L., DeRosset, W.S., and Helfritch, D., *Adiabatic shear instability based mechanism for particles/substrate bonding in the cold-gas dynamic-spray process.* Materials & Design, 2004. **25**(8): p. 681-688.

[5].Schmidt, T., Gaertner, F., and Kreye, H., *New developments in cold spray based on higher gas and particle temperatures.* Journal of Thermal Spray Technology, 2006. **15**(4): p. 488-494.

[6].Schmidt, T., Gartner, F., Assadi, H., and Kreye, H., *Development of a generalized parameter window for cold spray deposition.* Acta Materialia, 2006. **54**(3): p. 729-742.

[7].Assadi, H., Gartner, F., Stoltenhoff, T., and Kreye, H., *Bonding mechanism in cold gas spraying.* Acta Materialia, 2003. **51**(15): p. 4379-4394.

[8].GmbH, C.G.T. *CGT- Cold Gas Technology*. 2010 [cited 2010 Sep 27]; Available from: http://www.cgt-gmbh.com/.

[9].Inovati. *Inovati- Home of Kinetic Metallization*. 2010 [cited 2010 Sep 27]; Available from: http://www.inovati.com/.

[10]. Technology, S.S. *CenterLine Supersonic Spray Technology (SST)- Practical Cold Spray Solutions*. 2010 [cited 2010 Sep 27]; Available from: http://www.supersonicspray.com/.

[11]. Karthikeyan, J., *The Advantages and disadvantages of the cold spray coating process*, in *The cold spray materials deposition process : fundamentals and applications* V.K. Champagne, Editor 2007, Woodhead ; CRC Press. p. 62-71.

[12]. Wong, W., Irissou, E., Legoux, J.-G., and Yue, S., *Influence of helium and nitrogen gases on the properties of cold gas dynamic sprayed pure titanium coatings*, in *Thermal spray: Global Solutions for Future Application*, B.R. Marple, et al., Editors. 2010, ASM International: Singapore.

[13]. Borchers, C., Gartner, F., Stoltenhoff, T., Assadi, H., and Kreye, H., *Microstructural and macroscopic properties of cold sprayed copper coatings.* Journal of Applied Physics, 2003. **93**(12): p. 10064-10070.

[14]. Haynes, J., Pandey, A., Karthikeyan, J., and Kay, A., *Cold Sprayed Discontinuously Reinforced Alumina (DRA)* in *Thermal Spray: Building on 100 Years of Success*, B. R. Marple, et al., Editors. 2006, ASM International: Seattle, WA.

[15]. Koivuluoto, H., Näkki, J., and Vuoristo, P., *Corrosion Properties of Cold-Sprayed Tantalum Coatings.* Journal of Thermal Spray Technology, 2009. **18**(1): p. 75-82.

[16]. Balani, K., Laha, T., Agarwal, A., Karthikeyan, J., and Munroe, N., *Effect of carrier gases on microstructural and electrochemical behavior of cold-sprayed 1100 aluminum coating.* Surface & Coatings Technology, 2005. **195**(2-3): p. 272-279.

[17]. Dykhuizen, R.C. and Smith, M.F., *Gas dynamic principles of cold spray.* Journal of Thermal Spray Technology, 1998. **7**(2): p. 205-212.

[18]. Alkhimov, A., Kosarev, V., and Klinkov, S., *The features of cold spray nozzle design.* Journal of Thermal Spray Technology, 2001. **10**(2): p. 375-381.

[19]. Price, T.S., *Cold gas dynamic spraying of titanium coatings*, 2008, University of Nottingham.

[20]. Oosthuizen, P.H. and Carscallen, W.E., *Compressible fluid flow* McGraw-Hill series in aeronautical and aerospace engineering1997: McGraw-Hill.

[21]. Grujicic, M., Zhao, C.L., Tong, C., DeRosset, W.S., and Helfritch, D., *Analysis of the impact velocity of powder particles in the cold-gas dynamic-spray process.* Materials Science and Engineering A, 2004. **368**(1-2): p. 222-230.

[22]. Grujicic, M., Tong, C., DeRosset, W., and Helfritch, D., *Flow analysis and nozzle-shape optimization for the cold-gas dynamic-spray process.* Proceedings of the Institution of Mechanical Engineers, Part B: Journal of Engineering Manufacture, 2003. **217**(11): p. 1603-1613.

[23]. Van Steenkiste, T. and Smith, J.R., *Evaluation of coatings produced via kinetic and cold spray processes.* Journal of Thermal Spray Technology, 2004. **13**(2): p. 274-282.

[24]. Lee, J., Shin, S., Kim, H., and Lee, C., *Effect of gas temperature on critical velocity and deposition characteristics in kinetic spraying.* Applied Surface Science, 2007. **253**(7): p. 3512-3520.

[25]. Li, W.Y., Zhang, C., Guo, X.P., Zhang, G., Liao, H.L., Li, C.J., and Coddet, C., *Effect of standoff distance on coating deposition characteristics in cold spraying.* Materials & Design, 2008. **29**(2): p. 297-304.

[26]. Gartner, F., Stoltenhoff, T., Schmidt, T., and Kreye, H., *The cold spray process and its potential for industrial applications.* Journal of Thermal Spray Technology, 2006. **15**(2): p. 223-232.

[27]. Gilmore, D.L., Dykhuizen, R.C., Neiser, R.A., Roemer, T.J., and Smith, M.F., *Particle velocity and deposition efficiency in the cold spray process.* Journal of Thermal Spray Technology, 1999. **8**(4): p. 576-582.

[28]. Pattison, J., Celotto, S., Khan, A., and O'Neill, W., *Standoff distance and bow shock phenomena in the Cold Spray process.* Surface and Coatings Technology, 2008. **202**(8): p. 1443-1454.

[29]. Samareh, B., Stier, O., Lüthen, V., and Dolatabadi, A., *Assessment of CFD Modeling via Flow Visualization in Cold Spray Process.* Journal of Thermal Spray Technology, 2009. **18**(5): p. 934-943.

[30]. Stoltenhoff, T., Kreye, H., and Richter, H.J., *An analysis of the cold spray process and its coatings.* Journal of Thermal Spray Technology, 2002. **11**(4): p. 542-550.

[31]. Yin, S., Wang, X.-f., Li, W.-y., and Xu, B.-p., *Numerical Study on the Effect of Substrate Angle on Particle Impact Velocity and Normal Velocity Component in Cold Gas Dynamic Spraying Based on CFD.* Journal of Thermal Spray Technology.

[32]. Morgan, R., Fox, P., Pattison, J., Sutcliffe, C., and O'Neill, W., *Analysis of cold gas dynamically sprayed aluminium deposits.* Materials Letters, 2004. **58**(7-8): p. 1317-1320.

[33]. Bae, G., Kumar, S., Yoon, S., Kang, K., Na, H., Kim, H.-J., and Lee, C., *Bonding features and associated mechanisms in kinetic sprayed titanium coatings.* Acta Materialia, 2009. **57**(19): p. 5654-5666.

[34]. Bae, G., Xiong, Y., Kumar, S., Kang, K., and Lee, C., *General aspects of interface bonding in kinetic sprayed coatings.* Acta Materialia, 2008. **56**(17): p. 4858-4868.

[35]. Grujicic, M., Saylor, J.R., Beasley, D.E., DeRosset, W.S., and Helfritch, D., *Computational analysis of the interfacial bonding between feed-powder particles and the substrate in the cold-gas dynamic-spray process.* Applied Surface Science, 2003. **219**(3-4): p. 211-227.

[36]. Li, C.J., Li, W.Y., and Liao, H.L., *Examination of the critical velocity for deposition of particles in cold spraying.* Journal of Thermal Spray Technology, 2006. **15**(2): p. 212-222.

[37]. Li, W.Y., Liao, H.L., Li, C.J., Bang, H.S., and Coddet, C., *Numerical simulation of deformation behavior of Al particles impacting on Al substrate and effect of surface oxide films on interfacial bonding in cold spraying.* Applied Surface Science, 2007. **253**(11): p. 5084-5091.

[38]. Li, W.Y., Liao, H.L., Li, C.J., Li, G., Coddet, C., and Wang, X.F., *On high velocity impact of micro-sized metallic particles in cold spraying.* Applied Surface Science, 2006. **253**(5): p. 2852-2862.

[39]. Vlcek, J., Gimeno, L., Huber, H., and Lugscheider, E., *A systematic approach to material eligibility for the cold-spray process.* Journal of Thermal Spray Technology, 2005. **14**(1): p. 125-133.

[40]. Yokoyama, K., Watanabe, M., Kuroda, S., Gotoh, Y., Schmidt, T., and Gartner, F., *Simulation of Solid Particle Impact Behavior for Spray Processes.* Materials Transactions, 2006. **47**(7): p. 1697-1702.

[41]. King, P., Bae, G., Zahiri, S., Jahedi, M., and Lee, C., *An Experimental and Finite Element Study of Cold Spray Copper Impact onto Two Aluminum Substrates.* Journal of Thermal Spray Technology, 2010. **19**(3): p. 620-634.

[42]. Li, W.-Y., Zhang, C., Li, C.-J., and Liao, H., *Modeling Aspects of High Velocity Impact of Particles in Cold Spraying by Explicit Finite Element Analysis.* Journal of Thermal Spray Technology, 2009. **18**(5): p. 921-933.

[43]. Schmidt, T., Assadi, H., Gärtner, F., Richter, H., Stoltenhoff, T., Kreye, H., and Klassen, T., *From Particle Acceleration to Impact and Bonding in Cold Spraying.* Journal of Thermal Spray Technology, 2009. **18**(5): p. 794-808.

[44]. Assadi, H., Richter, H.J., Gartner, F., Schmidt, T., Stoltenhoff, T., Kreye, H., and Klassen, T., *Particle acceleration, impact and coating formation in cold spraying*, in *8th Colloquium High Velocity Oxy-fuel Flame Spray*, C. Penszior and P. Heinrich, Editors. 2009, Gemeinschaft Thermisches Spritzen e.V. (Association of Thermal Sprayers): Erding near Munich. p. 27-36.

[45]. Xiong, Y., Bae, G., Xiong, X., and Lee, C., *The Effects of Successive Impacts and Cold Welds on the Deposition Onset of Cold Spray Coatings.* Journal of Thermal Spray Technology. **19**(3): p. 575-585.

[46]. Guetta, S., Berger, M., Borit, F., Guipont, V., Jeandin, M., Boustie, M., Ichikawa, Y., Sakaguchi, K., and Ogawa, K., *Influence of Particle Velocity on Adhesion of Cold-Sprayed Splats.* Journal of Thermal Spray Technology, 2009. **18**(3): p. 331-342.

[47]. Johnson, G.R. and Cook, W.H., *Fracture characteristics of three metals subjected to various strains, strain rates, temperatures and pressures.* Engineering Fracture Mechanics, 1985. **21**(1): p. 31-48.

[48]. Conrad, H. and Rice, L., *The cohesion of previously fractured Fcc metals in ultrahigh vacuum.* Metallurgical and Materials Transactions B, 1970. **1**(11): p. 3019-3029.

[49]. Buckley, D.H. and Johnson, R.L., *The influence of crystal structure and some properties of hexagonal metals on friction and adhesion.* Wear, 1968. **11**(6): p. 405-419.
[50]. Klinkov, S.V., Kosarev, V.F., and Rein, M., *Cold spray deposition: Significance of particle impact phenomena.* Aerospace Science and Technology, 2005. **9**(7): p. 582-591.
[51]. Schmidt, T., Gartner, F., Kreye, H., and Klassen, T., *Correlation of particle impact conditions and coating properties in cold spraying*, in *Thermal Spray: Global Coating Solutions*, E. Lugscheider, Editor 2008, ASM International: Maastricht, The Netherlands. p. 724-731.
[52]. Yin, S., Wang, X.-f., Xu, B.-p., and Li, W.-y., *Examination on the Calculation Method for Modeling the Multi-Particle Impact Process in Cold Spraying.* Journal of Thermal Spray Technology.
[53]. Bae, G., Kang, K., Na, H., and Lee, C., *Thermally Enhanced Kinteic Sprayed Titanium Coating: Microstructure and Property Improvement for Potential Application*, in *Thermal Spray 2009: Expanding Thermal Spray Performance to New Markets and Applications*, B.R. Marple, et al., Editors. 2009, ASM International: Las Vegas, NV. p. 290-295.
[54]. Wu, J.W., Fang, H.Y., Yoon, S., Kim, H., and Lee, C., *The rebound phenomenon in kinetic spraying deposition.* Scripta Materialia, 2006. **54**(4): p. 665-669.
[55]. Kurochkin, Y.V., Demin, Y.N., and Soldatenkov, S.I., *Demonstration of the Method of Cold Gasdynamic Spraying of Coatings.* Chemical and Petroleum Engineering, 2002. **38**(3): p. 245-248.
[56]. Alkhimov, A., Klinkov, S., and Kosarev, V., *Experimental study of deformation and attachment of microparticles to an obstacle upon high-rate impact.* Journal of Applied Mechanics and Technical Physics, 2000. **41**(2): p. 245-250.
[57]. Barradas, S., Guipont, V., Molins, R., Jeandin, M., Arrigoni, M., Boustie, M., Bolis, C., Berthe, L., and Ducos, M., *Laser shock flier impact simulation of particle-substrate interactions in cold spray.* Journal of Thermal Spray Technology, 2007. **16**(4): p. 548-556.
[58]. Barradas, S., Molins, R., Jeandin, M., Arrigoni, M., Boustie, M., Bolis, C., Berthe, L., and Ducos, M., *Application of laser shock adhesion testing to the study of the interlamellar strength and coating-substrate adhesion in cold-sprayed copper coating of aluminum.* Surface and Coatings Technology, 2005. **197**(1): p. 18-27.
[59]. Champagne, V.K., Helfritch, D., Leyman, P., Ahl, S.G., and Klotz, B., *Interface material mixing formed by the deposition of copper on aluminum by means of the cold spray process.* Journal of Thermal Spray Technology, 2005. **14**(3): p. 330-334.
[60]. Christoulis, D.K., Borit, F., Guipont, F., and Jeandin, M., *Evidence of the 2-stage build-up process in cold spray from the study of influence of powder characteristics on Ti-6Al-4V coating*, in *Thermal Spray: Global Coating Solutions*, E. Lugscheider, Editor 2008, ASM International: Maastricht, The Netherlands.
[61]. Dykhuizen, R.C., Smith, M.F., Gilmore, D.L., Neiser, R.A., Jiang, X., and Sampath, S., *Impact of high velocity cold spray particles.* Journal of Thermal Spray Technology, 1999. **8**(4): p. 559-564.
[62]. Kang, K., Yoon, S., Ji, Y., and Lee, C., *Oxidation dependency of critical velocity for aluminum feedstock deposition in kinetic spraying process.* Materials Science and Engineering a-Structural Materials Properties Microstructure and Processing, 2008. **486**(1-2): p. 300-307.
[63]. Li, C.J., Wang, H.T., Zhang, Q., Yang, G.J., Li, W.Y., and Liao, H., *Influence of Spray Materials and Their Surface Oxidation on the Critical Velocity in Cold Spraying.* Journal of Thermal Spray Technology, 2010. **19 (1-2)**(1): p. 95-101.
[64]. Li, W., Guo, X., Yu, M., Liao, H., and Coddet, C., *Investigation of Impact Behavior of Cold-Sprayed Large Annealed Copper Particles and Characterization of Coatings.* Journal of Thermal Spray Technology.
[65]. Price, T.S., Shipway, P.H., McCartney, D.G., Calla, E., and Zhang, D., *A method for characterizing the degree of inter-particle bond formation in cold sprayed coatings.* Journal of Thermal Spray Technology, 2007. **16**(4): p. 566-570.

[66]. Shkodkin, A., Kashirin, A., Klyuev, O., and Buzdygar, T., *Metal particle deposition stimulation by surface abrasive treatment in gas dynamic spraying.* Journal of Thermal Spray Technology, 2006. **15**(3): p. 382-386.
[67]. Shukla, V., Elliott, G.S., Kear, B.H., and McCandlish, L.E., *Hyperkinetic deposition of nanopowders by supersonic rectangular jet impingement.* Scripta Materialia, 2001. **44**(8-9): p. 2179-2182.
[68]. Tokarev, A.O., *Structure of aluminum powder coatings prepared by cold gasdynamic spraying.* Metal Science and Heat Treatment, 1996. **38**(3-4): p. 136-139.
[69]. Van Steenkiste, T.H., Smith, J.R., and Teets, R.E., *Aluminum coatings via kinetic spray with relatively large powder particles.* Surface & Coatings Technology, 2002. **154**(2-3): p. 237-252.
[70]. Van Steenkiste, T.H., Smith, J.R., Teets, R.E., Moleski, J.J., Gorkiewicz, D.W., Tison, R.P., Marantz, D.R., Kowalsky, K.A., Riggs, W.L., Zajchowski, P.H., Pilsner, B., McCune, R.C., and Barnett, K.J., *Kinetic spray coatings.* Surface & Coatings Technology, 1999. **111**(1): p. 62-71.
[71]. Hussain, T., McCartney, D.G., and Shipway, P.H., *Impact phenomena in cold-spraying of titanium onto various ferrous alloys.* Surface and Coatings Technology, 2011. **205**(21-22): p. 5021-5027.
[72]. Hussain, T., McCartney, D.G., Shipway, P.H., and Zhang, D., *Bonding Mechanisms in Cold Spraying: The Contributions of Metallurgical and Mechanical Components.* Journal of Thermal Spray Technology, 2009. **18**(3): p. 364-379.
[73]. Hussain, T., McCartney, D.G., and Shipway, P.H., *Bonding between aluminium and copper in cold spraying: story of asymmetry.* Materials Science and Technology, 2012.
[74]. C.F.Rocheville, *Device for Treating the Surface of a Workpiece*,U.S. Patent 3,100,724, Aug 13, 1963.
[75]. Koivuluoto, H., Lagerbom, J., Kylmälahti, M., and Vuoristo, P., *Microstructure and Mechanical Properties of Low-Pressure Cold-Sprayed (LPCS) Coatings.* Journal of Thermal Spray Technology, 2008. **17**(5-6): p. 721-727.
[76]. Djordjevic, B.B. and Maev, R.G., *SIMATTM Application for Aerospace Corrosion Protection and Structural Repair*, in *Thermal Spray: Building on 100 Years of Success*, B. R. Marple, et al., Editors. 2006, ASM International: Seattle, WA.
[77]. Shkodkin, A., Kashirin, A., Klyuev, O., and Buzdygar, T., *The Basic Principles of DYMET Technology*, in *Thermal Spray: Building on 100 Years of Success*, B. R. Marple, et al., Editors. 2006, ASM International: Seattle, WA.
[78]. Papyrin, A.N., Klinkov, S.V., and Kosarev, V.F., *Effect of substrate activation on the process of cold spray coating formation*, in *Thermal spray: Exploring its surfacing potential*, E. Lugscheider, Editor 2005, ASM International: Basel, Switzerland.
[79]. Li, J.F., Agyakwa, P.A., Johnson, C.M., Zhang, D., Hussain, T., and McCartney, D.G., *Characterization and solderability of cold sprayed Sn-Cu coatings on Al and Cu substrates.* Surface and Coatings Technology, 2010. **204**(9-10): p. 1395-1404.
[80]. King, P., Zahiri, S., and Jahedi, M., *Copper particle impact onto aluminium by cold spray*, in *Thermal Spray: Global Coating Solutions*, E. Lugscheider, Editor 2008, ASM International: Maastricht, The Netherlands.
[81]. Balani, K., Agarwal, A., Seal, S., and Karthikeyan, J., *Transmission electron microscopy of cold sprayed 1100 aluminum coating.* Scripta Materialia, 2005. **53**(7): p. 845-850.
[82]. Marrocco, T., McCartney, D.G., Shipway, P.H., and Sturgeon, A.J., *Production of titanium deposits by cold-gas dynamic spray: Numerical modeling and experimental characterization.* Journal of Thermal Spray Technology, 2006. **15**(2): p. 263-272.
[83]. Wu, J.W., Yang, J.G., Fang, H.Y., Yoon, S., and Lee, C., *The bond strength of Al-Si coating on mild steel by kinetic spraying deposition.* Applied Surface Science, 2006. **252**(22): p. 7809-7814.
[84]. H. Mäkinen, J. Lagerbom, and P. Vuoristo, *Adhesion of Cold Sprayed Coatings: Effect of Powder, Substrate, and Heat Treatment*, in *Thermal Spray: Global Coating Solutions*, B.R. Marple, et al., Editors. 2007, ASM International: Beijing, People's Republic of China. p. 31-36.

[85]. K. Sakaki, T. Tajima, H. Li, S. Shinkai, and Y. Shimizu, *Influence of Substrate Conditions and Traverse Speed on Cold Sprayed Coatings*, in *Thermal Spray: Advances in Technology and Application* 2004, ASM International: Osaka, Japan. p. 358–362.

[86]. Richer, P., Jodoin, B., Taylor, K., Sansoucy, E., Johnson, M., and Ajdelsztajn, L., *Effect of particle geometry and substrate preparation in cold spray*, in *Thermal spray: Exploring it's surfacing potential*, E. Lugscheider, Editor 2005, ASM International: Basel, Switzerland.

[87]. Segall, A.E., Papyrin, A.N., Conway, J.C., and Shapiro, D. *A cold-gas spray coating process for enhancing titanium*. in *TMS Annual Meeting*. 1998. San Antonio, Texas: Minerals Metals Materials Soc.

[88]. Sun, J.F., Han, Y., and Cui, K., *Innovative fabrication of porous titanium coating on titanium by cold spraying and vacuum sintering.* Materials Letters, 2008. **62**(21-22): p. 3623-3625.

[89]. Dosta, S., Cinca, N., Garcia, J., Salito, A., and Guilemany, J.M., *Cold spray perspectives in Medical Engineering*, in *8th Colloquium High Velocity Oxy-fuel Flame Spray*, C. Penszior and P. Heinrich, Editors. 2009, Gemeinschaft Thermisches Spritzen e.V. (Association of Thermal Sprayers): Erding near Munich. p. 151-156.

[90]. Li, W.Y., Zhang, C., Wang, H.T., Guo, X.P., Liao, H.L., Li, C.J., and Coddet, C., *Significant influences of metal reactivity and oxide films at particle surfaces on coating microstructure in cold spraying.* Applied Surface Science, 2007. **253**(7): p. 3557-3562.

[91]. Li, C.-J. and Li, W.-Y., *Deposition characteristics of titanium coating in cold spraying.* Surface and Coatings Technology, 2003. **167**(2-3): p. 278-283.

[92]. Wong, W., Rezaeian, A., Irissou, E., Legoux, J.-G., and Yue, S., *Cold Spray Characteristics of Commercially Pure Ti and Ti-6Al-4V.* Advanced Materials Research, 2010. **89-91**: p. 639-644.

[93]. Wong, W., Rezaeian, A., Yue, S., and Legoux, J.G., *Effects of Gas Temperature, Gas Pressure and the Particle Characteristics on Cold Sprayed Pure Titanium Coatings*, in *Thermal Spray 2009: Expanding Thermal Spray Performance to New Markets and Applications*, B.R. Marple, et al., Editors. 2009, ASM International: Las Vegas, NV. p. 231-236.

[94]. Gulizia, S., Trentin, A., Vezzu, S., Rech, S., King, P., Jahedi, M., and Guagliano, M., *Microstucture and Mechanical Properties of Cold spray Titanium Coatings*, in *Thermal spray: Global Solutions for Future Application*, B.R. Marple, et al., Editors. 2010, ASM International: Singapore.

[95]. Grenier, S., Brzezinski, T., Allaire, F., and Tsantrizos, P., *VPS Deposition of Spherical Ti-Based Powders Produced by Plasma Atomization* in *Thermal Spray: Meeting the Challenges of the 21st Century*, C. Coddet, Editor 1998, ASM International: Nice, France. p. 1277-1282.

[96]. Yule, A.J. and Dunkley, J.J., *Atomization of melts : for powder production and spray deposition* Oxford series on advanced manufacturing ; 111994: Oxford University Press.

[97]. Alagheband, A. and Brown, C., *Plasma Atomization goes commercial.* Metal Powder Report, 1998. **53**(11): p. 26-28.

[98]. Blose, R.E., *Spray Forming Titanium Alloys Using the Cold Spray Process.*, in *Thermal spray: Exploring its surfacing potential*, E. Lugscheider, Editor 2005, ASM International: Basel, Switzerland.

[99]. Blose, R.E., Walker, B.H., Walker, R.M., and Froes, S.H., *New opportunities to use cold spray process for applying additive features to titanium alloys.* Metal Powder Report, 2006. **61**(9): p. 30-37.

[100]. Blose, R.E., Walker, B.H., Walker, R.M., and Froes, S.H., *Depositing Titanium Alloy Additive Features to Forgings and Extrusions Using the Cold Spray Process*, in *Thermal Spray: Building on 100 Years of Success*, B. R. Marple, et al., Editors. 2006, ASM International: Seattle, WA.

[101]. Hussain, T., *A Study of Bonding Mechanisms and Corrosion Behaviour of Cold Sprayed Coatings*2011: University of Nottingham. 295.

[102]. Razaeian, A., Chromik, R.R., Yue, S., Irissou, E., and Legoux, J.G., *Characterization of cold-sprayed Ni, Ti and Cu coating properties for their optimizations*, in *Thermal Spray: Global Coating Solutions*, E. Lugscheider, Editor 2008, ASM International: Maastricht, The Netherlands.

[103]. Zahiri, S.H., Jahedi, M., and Yang, W., *Particle image velocimetry of cold spray CP titanium*, in *Thermal Spray: Global Coating Solutions*, E. Lugscheider, Editor 2008, ASM International: Maastricht, The Netherlands.

[104]. Chromik, R.R., Goldbaum, D., Shockley, J.M., Yue, S., Irissou, E., Legoux, J.-G., and Randall, N.X., *Modified ball bond shear test for determination of adhesion strength of cold spray splats.* Surface and Coatings Technology, 2010. **205**(5): p. 1409-1414.

[105]. Lima, R.S., Kucuk, A., Berndt, C.C., Karthikeyan, J., Kay, C.M., and Lindemann, J., *Deposition efficiency, mechanical properties and coating roughness in cold-sprayed titanium.* Journal of Materials Science Letters, 2002. **21**(21): p. 1687-1689.

[106]. Zahiri, S.H., Yang, W., and Jahedi, M., *Characterization of Cold Spray Titanium Supersonic Jet.* Journal of Thermal Spray Technology, 2009. **18**(1): p. 110-117.

[107]. Wang, H.-R., Hou, B.-R., Wang, J., Wang, Q., and Li, W.-Y., *Effect of Process Conditions on Microstructure and Corrosion Resistance of Cold-Sprayed Ti Coatings.* Journal of Thermal Spray Technology, 2008. **17**(5): p. 736-741.

[108]. Li, W.Y., Zhang, C., Guo, X.P., Li, C.J., Liao, H.L., and Coddet, C., *Study on impact fusion at particle interfaces and its effect on coating microstructure in cold spraying.* Applied Surface Science, 2007. **254**(2): p. 517-526.

[109]. Price, T.S., Shipway, P.H., and McCartney, D.G., *Effect of cold spray deposition of a titanium coating on fatigue behavior of a titanium alloy.* Journal of Thermal Spray Technology, 2006. **15**(4): p. 507-512.

[110]. Zahiri, S.H., Antonio, C.L., and Jahedi, M., *Elimination of porosity in directly fabricated titanium via cold gas dynamic spraying.* Journal of Materials Processing Technology, 2009. **209**(2): p. 922-929.

[111]. Zahiri, S.H., Mayo, S.C., and Jahedi, M., *Characterization of cold spray titanium deposits by X-ray microscopy and microtomography.* Microscopy and Microanalysis, 2008. **14**(3): p. 260-266.

[112. Ilavsky, J., *Characterization of Complex Thermal Barrier Deposits Pore Microstructures by a Combination of Imaging, Scattering, and Intrusion Techniques.* Journal of Thermal Spray Technology, 2010. **19**(1): p. 178-189.

[113]. Hussain, T., McCartney, D.G., Shipway, P.H., and Marrocco, T., *Corrosion Behavior of Cold Sprayed Titanium Coatings and Free Standing Deposits.* Journal of Thermal Spray Technology, 2011. **20**(1-2): p. 260-274.

[114]. Moy, C.K.S., Cairney, J., Ranzi, G., Jahedi, M., and Ringer, S.P., *Investigating the microstructure and composition of cold gas-dynamic spray (CGDS) Ti powder deposited on Al 6063 substrate.* Surface and Coatings Technology, 2010. **204**(23): p. 3739-3749.

[115]. Zahiri, S.H., Fraser, D., and Jahedi, M., *Recrystallization of Cold Spray-Fabricated CP Titanium Structures.* Journal of Thermal Spray Technology, 2009. **18**(1): p. 16-22.

[116]. Li, W.Y., Zhang, C., Guo, X., Xu, J., Li, C.J., Liao, H., Coddet, C., and Khor, K.A., *Ti and Ti-6Al-4V Coatings by Cold Spraying and Microstructure Modification by Heat Treatment.* Advanced Engineering Materials, 2007. **9**(5): p. 418-423.

[117]. Gulizia, S., Tiganis, B., Jahedi, M.Z., Wright, N., Gengenbach, T., and MacRae, C., *Effects of Cold Spray Process Gas Temperature on CP Titanium Structure*, in *Thermal Spray 2009: Expanding Thermal Spray Performance to New Markets and Applications*, B.R. Marple, et al., Editors. 2009, ASM International: Las Vegas, NV. p. 237-242.

[118]. King, P.C. and Jahedi, M., *Transmission electron microscopy of cold sprayed titanium*, in *Thermal spray: Global Solutions for Future Application*, B.R. Marple, et al., Editors. 2010, ASM International: Singapore. p. May 3- 5.

[119]. Bae, G., Kang, K., Kim, J.-J., and Lee, C., *Nanostructure formation and its effects on the mechanical properties of kinetic sprayed titanium coating.* Materials Science and Engineering: A, 2010. **527**(23): p. 6313-6319.
[120]. Cullity, B.D. and Stock, S.R., *Elements of X-ray diffraction* 2001: Prentice Hall.
[121]. Rafaja, D., Schucknecht, T., Klemm, V., Paul, A., and Berek, H., *Microstructural characterisation of titanium coatings deposited using cold gas spraying on Al2O3 substrates.* Surface and Coatings Technology, 2009. **203**(20-21): p. 3206-3213.
[122]. Watts, J.F. and Wolstenholme, J., *An introduction to surface analysis by XPS and AES*2003: J. Wiley.
[123]. Binder, K., Gartner, F., and Klassen, T., *Ti-Parts for Aviation Industry produced by Cold Spraying*, in *Thermal spray: Global Solutions for Future Application*, B.R. Marple, et al., Editors. 2010, ASM International: Singapore.
[124]. Jazi, H.R.S., Coyle, T.W., and Mostaghimi, J., *Understanding grain growth and pore elimination in vacuum-plasma-sprayed titanium alloy.* Metallurgical and Materials Transactions A-Physical Metallurgy and Materials Science, 2007. **38A**(3): p. 476-484.
[125]. Li, C.-j. and Li, W.-y., *Microstructure evolution of cold-sprayed coating during deposition and through post-spraying heat treatment.* Transactions of Nonferrous Metals Society of China 2004. **14**(2): p. 49-55.
[126]. Marrocco, T., Hussain, T., McCartney, D.G., and Shipway, P.H., *Corrosion Performance of Laser Posttreated Cold Sprayed Titanium Coatings.* Journal of Thermal Spray Technology, 2011. **20**(4): p. 909-917.
[127]. Kim, K., Watanabe, M., Kawakita, J., and Kuroda, S., *Effects of Temperature of In-flight Particles on Bonding and Microstructure in Warm-Sprayed Titanium Deposits.* Journal of Thermal Spray Technology, 2009.
[128]. Kim, K., Watanabe, M., Kawakita, J., and Kuroda, S., *Grain refinement in a single titanium powder particle impacted at high velocity.* Scripta Materialia, 2008. **59**(7): p. 768-771.
[129]. Kim, K., Watanabe, M., and Kuroda, S., *Bonding mechanisms of thermally softened metallic powder particles and substrates impacted at high velocity.* Surface and Coatings Technology, 2010. **204**(14): p. 2175-2180.
[130]. Kim, K., Watanabe, M., and Kuroda, S., *Thermal softening effect on the deposition efficiency and microstructure of warm sprayed metallic powder.* Scripta Materialia, 2009. **60**(8): p. 710-713.
[131]. Kim, K., Watanabe, M., and Kuroda, S., *Jetting-Out Phenomenon Associated with Bonding of Warm-Sprayed Titanium Particles onto Steel Substrate.* Journal of Thermal Spray Technology, 2009. **18**(4): p. 490-499.
[132]. Kim, K., Watanabe, M., Mitsuishi, K., Iakoubovskii, K., and Kuroda, S., *Impact bonding and rebounding between kinetically sprayed titanium particle and steel substrate revealed by high-resolution electron microscopy.* Journal of Physics D-Applied Physics, 2009. **42**(6): p. 5.
[133]. Kawakita , J., Watanabe, M., and Kuroda, S., *Densification of Ti Coatings by Bi-modal Size Distribution of Feedstock Powder during Warm Spraying*, in *Thermal Spray: Global Coating Solutions*, B.R. Marple, et al., Editors. 2007, ASM International: Beijing, People's Republic of China. p. 43-47.
[134]. Deng, C.M., Deng, C.G., Liu, M., Huang, J., Zhou, K.S., Chen, Z.K., Wank, A., and Schwenk, A., *Corrosion of Ti coating prepared by modified HVOF process*, in *Thermal spray: Global Solutions for Future Application*, B.R. Marple, et al., Editors. 2010, ASM International: Singapore.
[135]. Kawakita, J., Kuroda, S., Fukushima, T., Katanoda, H., Matsuo, K., and Fukanuma, H., *Dense titanium coatings by modified HVOF spraying.* Surface & Coatings Technology, 2006. **201**(3-4): p. 1250-1255.

Progress in Surface Treatment II
10.4028/www.scientific.net/KEM.533

Cold Spraying of Titanium: A Review of Bonding Mechanisms, Microstructure and Properties
10.4028/www.scientific.net/KEM.533.53